Exact WKB and the quantum Seiberg-Witten curve for 4d $N = 2$ pure $\mathrm{SU}(3)$ Yang-Mills. Abelianization

Fei Yan

NHETC and Department of Physics and Astronomy, Rutgers University,
136 Frelinghuysen Rd, Piscataway, NJ 08854, U.S.A.

E-mail: fyan.hepth@gmail.com

ABSTRACT: We investigate the exact WKB method for the quantum Seiberg-Witten curve of 4d $N = 2$ pure SU(3) Yang-Mills in the language of abelianization. The relevant differential equation is a third-order equation on $\mathbb{CP}^1$ with two irregular singularities. We employ the exact WKB method to study the solutions to such a third-order equation and the associated Stokes phenomena. We also investigate the exact quantization condition for a certain spectral problem. Moreover, exact WKB analysis leads us to consider new Darboux coordinates on a moduli space of flat SL(3,$\mathbb{C}$)-connections. In particular, in the weak coupling region we encounter coordinates of the higher length-twist type generalizing Fenchel-Nielsen coordinates. The Darboux coordinates are conjectured to admit asymptotic expansions given by the formal quantum periods series and we perform numerical analysis supporting this conjecture.

Contents

1 Introduction

Recently there has been significant progress in the application of resurgence theory and exact WKB analysis to quantum mechanics (e.g. [1–15]). Simultaneously, many interesting relations have been discovered between quantum mechanical systems and supersymmetric gauge theories (e.g. [16–39]). The discovered relationships provide various tools to study the quantum mechanical problems in the context of quantization of Seiberg-Witten curves [40, 41] in certain 4d $N = 2$ theories. Furthermore these relationships have proven

useful in the study of differential equations appearing in various different contexts, as an example see the recent developments in applying Seiberg-Witten techniques to black hole perturbation theory [42–45].

Previous work has primarily focused on the study of second order differential equations such as the Schrödinger equation, in examples where the equation could be interpreted as the quantum Seiberg-Witten curve in a certain rank one 4d N=2 gauge theory. An interesting and important direction is to generalize such analyses to higher rank gauge theories whose quantum Seiberg-Witten curves could be higher order differential equations. Similar to the Schrödinger equation, such higher order differential equations have intrinsic meanings from the viewpoint of higher rank 4d $N = 2$ theories and their associated integrable systems.[1] Furthermore, techniques developed to study higher rank 4d $N = 2$ theories may benefit the study of higher order differential equations appearing elsewhere in physics and mathematics.

Our goal in this paper and its follow up [47] is to study the quantum Seiberg-Witten curve of a 4d $N = 2$ pure SU(3) super Yang-Mills (SYM) theory via different approaches. We hope our results not only benefit the study of super Yang-Mills theories, but also sheds light on the exact WKB analysis for higher order Schrödinger-like equations.

1.1 Supersymmetric gauge theories and quantum mechanical systems

We begin with a review of correspondences between supersymmetric gauge theories and quantum mechanical systems from three different perspectives.

1.1.1 The gauge/Bethe correspondence

The first perspective arises in the context of gauge/Bethe correspondence [16, 48, 49] in which 4d $N = 2$ gauge theories in the Ω-background provide the quantization of certain classical integrable systems. Concretely, one takes the Nekrasov-Shatashvili (NS) limit with $\epsilon_1 = \hbar$ and $\epsilon_2 \to 0$ yielding the low energy effective 2d $N = (2,2)$ theory with an effective twisted superpotential given by:

$$\widetilde{W}_{\text{eff}}(\mathbf{a}, \hbar) = \lim_{\epsilon_2 \to 0} \epsilon_2 \log Z(\mathbf{a}, \epsilon_1 = \hbar, \epsilon_2), \tag{1.1}$$

where $Z(\mathbf{a}, \epsilon_1, \epsilon_2)$ is the 4d Nekrasov partition function in the Ω-background [50, 51]. We have denoted the vacuum expectation values of complex scalars in the $N = 2$ vector multiplets by $\mathbf{a}$. The effective 2d theory has a discrete set of vacua corresponding to solutions of

$$\exp\left(\frac{\partial \widetilde{W}_{\text{eff}}(\mathbf{a}, \hbar)}{\partial a_i}\right) = 1, \quad i = 1, \dots, r \tag{1.2}$$

where r is the rank of the 4d theory. In the context of quantum integrable systems, $\widetilde{W}_{\text{eff}}(\mathbf{a}, \hbar)$ is identified with the Yang-Yang functional, and equation (1.2) is the Bethe equation determining the set of eigenvalues of mutually commuting Hamiltonians.

---

[1] For example, these higher order differential equations are satisfied by the regular part of the partition function of the corresponding gauge theories with the insertion of a canonical surface defect in the Nekrasov-Shatashvili limit of the Omega background [46].

There is a special class of 4d $N = 2$ theories called class S theories $\mathcal{T}(\mathfrak{g}, C)$ which are obtained by compactifying the 6d $(2,0)$ theory of type $\mathfrak{g}$ on a Riemann surface C with a partial topological twist [52, 53]. Subjecting a class S theory to Ω-deformation in the NS limit [16, 54] gives quantization of the corresponding Hitchin integrable system where the corresponding phase space is the moduli space $\mathcal{M}_H(\mathfrak{g}, C)$,[2] of solutions to Hitchin's equations on the Riemann surface C [55].

In this context, the Seiberg-Witten curve of the class S theory is quantized to an *oper* [56], which is a certain meromorphic differential operator on C. As an example consider the case of $\mathfrak{g} = A_{N-1}$, an oper in a class S theory of type A_{N-1} could be locally written as the following N-th order meromorphic operator on C:

$$\mathcal{O}_N(z) := \partial_z^N + t_2(z, \hbar)\partial_z^{N-2} + \cdots + t_N(z, \hbar). \tag{1.3}$$

Moreover, the variety of opers is an $\hbar$-dependent Lagrangian submanifold in $\mathcal{M}_H(\mathfrak{g}, C, \hbar)$ which provides the quantization of Coulomb branch of the class S theory.

In [18] it was proposed that, for a class S theory $\mathcal{T}(A_{N-1}, C)$, there exists a specific Darboux coordinate system in which the generating function for the variety of opers is identified with the effective twisted superpotential up to certain boundary contribution at infinity. This is often called the NRS conjecture. As studied in [18], for $N = 2$ such coordinates are complexified Fenchel-Nielsen coordinates [57]. Some examples of $N > 2$ have been explored in [46, 58], where the relevant Darboux coordinates are higher-rank analoges of Fenchel-Nielsen coordinates. In particular, [46] gave a gauge-theoretic derivation of NRS conjecture and its generalization to a certain A_2 class-S theory by studying certain 1/2-BPS codimension-two surface defects in the 4d theory. Concretely, the non-perturbative Dyson-Schwinger equation [22] satisfied by the surface defect partition function in the Ω-background gives a quantized version of opers which reduces to the oper equation in the NS limit.

1.1.2 The topological string/spectral theory correspondence

Another interesting development is the topological string/spectral theory (TS/ST) correspondence [20, 21, 59] which associates a non-perturbative quantum mechanical operator to a toric Calabi-Yau manifold. The relevant spectral problem is associated with the quantization scheme for mirror curves to the toric Calabi-Yau manifold. In particular, explicit expressions for the spectral determinant could be written down using an 11d version of the topological string free energy [20] which allows for the derivation of exact quantization conditions for the operator spectrum.

To make contact with 4d $N = 2$ theories, one uses geometric engineering methods [60] by taking a certain limit of the topological string theory on the appropriate Calabi-Yau geometry [32, 61]. Quantization of the Seiberg-Witten curve arises as the *canonical quantization* of an algebraic curve. As an example, [61] studied a deformed Hamiltonian in quantum mechanics which arises in the context of the quantization of Seiberg-Witten curves

---

[2]Here one needs to specify the global form of the gauge group G corresponding to the Lie algebra $\mathfrak{g}$. In this article we consider $\mathfrak{g} = sl(N)$ and $G = \mathrm{SU}(N)$.

(as hyperelliptic curves [40, 62–64]) for 4d $N = 2$ pure SU(N) SYM. A conjectural exact quantization condition was written down in closed form, using the 4d limit of TS/ST correspondence.

1.1.3 Opers and the conformal limit

There is yet another way, introduced in [19], to describe the quantization of the Coulomb branch of class S theories in terms of the variety of opers.

As described in [52], compactifying a class S theory $\mathcal{T}(\mathfrak{g}, C)$ on a circle with radius R yield a low energy effective theory which is a 3d $N = 4$ sigma model with target space being a Hitchin moduli space $\mathcal{M}_H(\mathfrak{g}, C)$. Note that the radius R of the compactification circle is a parameter in the corresponding Hitchin's equations. $\mathcal{M}_H(\mathfrak{g}, C)$ has a $\mathbb{CP}^1$-worth of complex structures parametrized by ζ, where at $\zeta = 0$ the moduli space is a complex integrable system. It is described as a torus fibration over the Coulomb branch of the 4d theory, where the torus fibre parameterize the choice of Wilson lines and 't Hooft lines around the circle. With respect to the complex structure at $\zeta = 0$, there is a canonical Lagrangian submanifold $\mathcal{L}$ corresponding to the locus in $\mathcal{M}_H(\mathfrak{g}, C)$ where the Wilson and 't Hooft lines are turned off. $\mathcal{L}$ is canonically isomorphic to the 4d Coulomb branch.

The quantization of 4d Coulomb branch in this setup happens in a special scaling limit, the so-called *conformal limit* [19], where one sends both ζ and R to zero while keeping $\hbar = \zeta/R$ fixed. Viewing $\mathcal{M}_H(\mathfrak{g}, C)$ as a complex symplectic manifold in complex structure ζ, the conformal limit is a well-defined scaling limit and one denotes the resulting complex symplectic manifold as $\mathcal{M}_H(\mathfrak{g}, C; \hbar)$. Let $\mathcal{L}_\hbar$ be the image of $\mathcal{L}$ under the conformal limit, the statement is that $\mathcal{L}_\hbar$ is a Lagrangian submanifold in $\mathcal{M}_H(\mathfrak{g}, C; \hbar)$ and furthermore it was conjectured to coincide with the variety of opers. The physical motivation behind this conjecture was through twisted compactification of the 4d theory on $\Omega_\hbar$-deformed cigar-like geometry [54], where $\mathcal{L}_\hbar$ is related to the boundary condition at the tip of the cigar. This conjecture was demonstrated to be true in various examples in [19] and subsequent work such as [29, 31, 32, 38, 65–67]. From a mathematical point of view, this conjecture was proven in some special cases in [68].

From a computational point of view, the conjecture in [19] offers new insights into the study of quantum Seiberg Witten curves of class S theories. In particular, the conformal limit connects the exact WKB methods for opers with the exact WKB methods for flat connections parametrized by R and ζ. These methods were developed in [52, 69]. Concretely, the Stokes graphs appearing in exact WKB for opers are the same as the *spectral networks* introduced in [69]. As a result, techniques from the study of spectral networks could be directly applied to the exact WKB analysis for the Schrödinger equation and its higher order analogues. This philosophy was further explored in [31] which described the exact WKB method in the language of abelianization. We will give an overview of the method in section 2.

1.2 Different methods to compute resummed quantum periods

In section 1.1 we reviewed three setups where the quantization of Seiberg-Witten curves occurs motivating different methods to compute the corresponding properly resummed

quantum periods. Computing quantum periods using these different methods and verifying their agreement plays an important role in understanding the correspondences between 4d $N = 2$ gauge theories and quantum mechanical systems. Recently such checks have been performed in 4d $N = 2$ SU(2) SYM without or with matter content, see [11, 23–25, 28, 32, 38, 70–73] for example. In this paper and [47] our objective is to generalize such analysis to higher rank theories, using 4d $N = 2$ pure SU(3) SYM as a concrete example.

Let us consider the quantum Seiberg-Witten curve for a class S theory $\mathcal{T}(A_{N-1}, C)$ with associated differential equation corresponding to an SL(N)-oper in (1.3):

$$\left[\partial_z^N + t_2(z, \hbar)\partial_z^{N-2} + \cdots + t_N(z, \hbar)\right]\psi(z) = 0. \tag{1.4}$$

The standard WKB method makes the following ansatz for the wavefunction $\psi(z)$:

$$\psi(z) = \exp\left(\frac{1}{\hbar}\int_{z_0}^z \lambda(z)dz\right). \tag{1.5}$$

Substituting (1.5) into (1.4) yields an order-N analogue of the Riccati equation. The first step in constructing a solution is building a formal series solution to the Riccati equation in powers of $\hbar$. At order-$\hbar^0$, the relevant equation describes the classical Seiberg-Witten curve for $\mathcal{T}(A_{N-1}, C)$ as an N-fold branched covering $\widetilde{C} \to C$. There are N choices of order-$\hbar^0$ solutions corresponding to the N sheets of the Seiberg-Witten curve $\widetilde{C}$. We choose a sheet i and consider the formal series solution

$$\lambda_i^{\text{formal}}(\hbar) = \sum_{n=0}^{\infty} \lambda_i^{(n)}\hbar^n, \tag{1.6}$$

where $\lambda_i^{(0)}$ is an order-$\hbar^0$ solution. The higher order $\lambda_i^{(n)}$ are then uniquely fixed by recursively solving the Riccati equation in orders of $\hbar$.

Classical periods of the Seiberg-Witten curve are given by the integrals of $\lambda^{(0)}$ along 1-cycles γ of $\widetilde{C}$, where γ labels the IR electromagnetic (and flavor) charge. Correspondingly, the quantum periods or WKB periods are defined as

$$\Pi_\gamma(\hbar) := \oint_\gamma \lambda^{\text{formal}}(\hbar)dz, \quad \gamma \in H_1(\widetilde{C}, \mathbb{Z}), \tag{1.7}$$

where $\Pi_\gamma(\hbar)$ is a formal power series in $\hbar$

$$\Pi_\gamma(\hbar) = \sum_{n=0}^{\infty} \Pi_\gamma^{(n)}\hbar^n, \quad \Pi_\gamma^{(n)} = \oint_\gamma \lambda^{(n)}dz. \tag{1.8}$$

$\Pi_\gamma^{(n)}$ in general diverges as $n!$ [23, 32, 72, 74, 75]. An approach for properly resumming $\Pi_\gamma(\hbar)$ is the Borel resummation. There could be rays in the Borel plane along which the Borel transform has singularities. As a consequence, $\Pi_\gamma(\hbar)$ is not Borel summable for certain phases of $\hbar$. One could nevertheless define lateral Borel resummations by slightly deforming the integration contour below or above the ray corresponding to such a phase. These two choices of deformation produce different answers, where the difference is defined

as the *Stokes discontinuity* of quantum periods. Borel resummation of quantum periods and their associated Stokes discontinuities have a very rich structure which has been an important topic in resurgence theory, see for example [76].

The correspondences between gauge theories and quantum mechanical systems reviewed in section 1.1 motivates alternative ways to compute the resummed quantum periods, which we describe below.

1.2.1 Computing quantum periods via abelianization

Motivated by developments reviewed in section 1.1.3, the exact WKB method could be reformulated geometrically in the context of *abelianization* [31, 58, 69, 77]. Abelianization maps a flat SL(N,$\mathbb{C}$)-connection over the Riemann surface C to a flat GL(1,$\mathbb{C}$)-connection over the Seiberg-Witten curve $\widetilde{C} \to C$. The Borel resummed quantum periods are closely related to the *Voros symbols* $\mathcal{X}_\gamma(\hbar)$,[3] defined as the holonomy of the flat abelian connection along 1-cycles γ in $\widetilde{C}$.

Using abelianization methods, $\mathcal{X}_\gamma(\hbar)$ can be explicitly written as products of Wronskians of distinguished local solutions to the oper equation (1.4). In this way, $\mathcal{X}_\gamma(\hbar)$ could be identified as *spectral coordinates* on a moduli space of flat SL(N,$\mathbb{C}$)-connections. For the case of SL(2)-opers, $\mathcal{X}_\gamma(\hbar)$ are Fock-Goncharov coordinates in generic situations [52, 78]. In certain cases one could also obtain exponentiated complexified Fenchel-Nielsen coordinates [18, 57, 77]. For the case of higher-rank SL(N)-opers, $\mathcal{X}_\gamma(\hbar)$ could be identified with higher-rank Fock-Goncharov coordinates [69, 78] in special cases or higher length-twist coordinates [46, 58] generalizing Fenchel-Nielsen coordinates. In general though, abelianization for higher-rank opers yield spectral coordinates that haven't been studied in detail previously.

The connection between $\mathcal{X}_\gamma(\hbar)$ and the quantum periods is mediated by certain asymptotic properties of $\mathcal{X}_\gamma(\hbar)$ motivated from [19, 31, 52, 69]. In particular, as $\hbar \to 0$ while staying within a certain half of the $\hbar$-plane, $\log(\mathcal{X}_\gamma(\hbar))$ admits an asymptotic expansion

$$\log(\mathcal{X}_\gamma(\hbar)) \sim \frac{1}{\hbar}\Pi_\gamma(\hbar), \tag{1.9}$$

where $\Pi_\gamma(\hbar)$ is the formal series of quantum periods defined in (1.7). Moreover, if $\hbar \to 0$ along the central ray within the half-plane, $\hbar\log(\mathcal{X}_\gamma(\hbar))$ produces the Borel resummed quantum periods.[4]

For SL(2)-opers, mathematically such asymptotic behavior of Voros symbols has been proven by Koike-Schäfke and further studied by [79–81]. For higher SL(N)-opers it remains to be a conjecture. Certain numerical evidence for this conjecture in the higher rank case has been provided in [31, 67]. In this paper we provide further evidence in the concrete example of an SL(3)-oper which appears in the quantization of the Seiberg-Witten curve of the 4d $N = 2$ pure SU(3) SYM theory.

---

[3]More precisely, the Voros symbol depends on a phase parameter θ. Detailed definitions are described in section 2.

[4]If $\Pi_\gamma(\hbar)$ happens to be not Borel-summable, then $\hbar\log(\mathcal{X}_\gamma(\hbar))$ is conjectured to produce the median Borel summation of $\Pi_\gamma(\hbar)$ [31].

1.2.2 Computing quantum periods via TBA-like integral equations

The spectral coordinates $\mathcal{X}_\gamma(\hbar)$ obey certain TBA-like integral equations [19], which could be viewed as the conformal limit of the TBA-like integral equations in [82]. Such integral equations are determined by the BPS spectrum of the corresponding 4d $N = 2$ theory and are very useful in the study of quantum periods.

There exists an interesting correspondence between BPS states and the resurgent properties of quantum periods [19, 29, 32, 66]. Singularities of the Borel transform for quantum periods are controlled by the BPS spectrum of the 4d theory. Moreover, the Stokes discontinuities of quantum periods are closely related to the Kontsevich-Soibelman transformation [52, 82, 83]. As a consequence, the BPS spectrum and subsequently the integral equations predict the locations of singularities in the Borel plane and the discontinuites in lateral Borel resummations of quantum periods.

The Borel resummed quantum periods are solutions to the integral equations. In principal, one can compute them by solving the integral equations iteratively, after specifying appropriate boundary conditions on the solutions. This perspective has been explored in various examples in [19, 20, 29, 31, 32, 67]. In [47], we will provide numerical calculation of resummed quantum periods using the integral equations.

1.2.3 Computing quantum periods via instanton calculus

The NS limit [16] of instanton calculus [50, 51] also provides a resummation of quantum periods [32, 70]. Concretely, instanton calculus picks up distinguished quantum periods: the quantum A- and B-periods $\{a_1(\hbar), \ldots, a_r(\hbar), a_D^1(\hbar), \ldots, a_D^r(\hbar)\}$,[5] satisfying the quantum special geometry relation

$$a_D^i(a_1, \ldots, a_r; \hbar) = \frac{\partial F_{\mathrm{NS}}(a_1, \ldots, a_r; \hbar)}{\partial a_i}, \quad i = 1, \ldots, r \tag{1.10}$$

We have denoted the Nekrasov-Shatashvili free energy [16] by $F_{\mathrm{NS}}(a_1, \ldots, a_r; \hbar)$, which is $\hbar$ times the effective twisted superpotential $\widetilde{W}_{\mathrm{eff}}$. This free energy is given as a power series in the instanton counting parameter with a non-vanishing convergence radius in a certain parameter range around the semiclassical region.

Given the NS free energy, the quantum A-periods $a_i(\hbar)$ could be obtained by inverting the quantum Matone relation [23, 26, 27, 84–89]. The quantum B-periods $a_D^i(\hbar)$ are then computed via (1.10). For appropriate parameter range, both $a_i(\hbar)$ and $a_D^i(\hbar)$ are convergent series expansion in the instanton counting parameter with non-zero convergence radius, in particular they are exact in $\hbar$. Instanton calculus thus provides a natural resummation for the quantum A- and B-periods.[6]

The NRS conjecture and its higher rank generalization [18, 46, 58] suggests that the instanton resummed quantum A- and B-periods correspond to certain special spectral coordinates: the Fenchel-Nielsen coordinates or higher length-twist coordinates. Symbolically[7]

---

[5]Here r denotes the rank of the theory.

[6]The relationship between instanton resummation and Borel resummation has been clarified in [32] in the context of $N = 2$ pure SU(2) SYM.

[7]There are certain ambiguities in FN or higher length-twist coordinates corresponding to a certain monodromy action mixing a with a_D. We thank Andrew Neitzke for discussions on this.

one expects the following relation in the higher rank case:

$$\log\left(\mathcal{X}_\gamma^{\text{length}}(\hbar)\right) = \frac{1}{\hbar}a(\hbar), \quad \log\left(\mathcal{X}_\gamma^{\text{twist}}(\hbar)\right) = \frac{1}{\hbar}a_D(\hbar). \tag{1.11}$$

1.3 The canonical quantization and surface defects

Thus far we have avoided talking about an important issue in the quantization of Seiberg-Witten curves. In principal there could be different quantization choices which reduce to the same classical Seiberg-Witten curve. A natural question would be which choice corresponds to the *canonical* quantization where observables such as the Borel resummed quantum periods agree with predictions from TBA equations and instanton calculus. There has been many discussions on the canonical quantum Seiberg-Witten curve from gauge theory considerations [16, 17, 23–26, 28, 39, 46, 54, 61, 70, 90–100]. In [47], we derive such a canonical quantization using the canonical surface defect instanton partition function following similar methods as [46]. Concretely, one first computes the surface defect partition function in the full Omega background. Taking the Nekrasov-Shatashvili limit and extracting the regular part of the partition function then yields wavefunctions satisfying a certain differential equation. This differential equation is regarded as the canonical quantum Seiberg-Witten curve, in the sense that it has a natural gauge theory interpretation. As a further remark, the canonical surface defect also plays an important role in the exact WKB analysis for the quantum Seiberg-Witten curve. In particular, the soliton spectrum of the surface defect determines the Stokes curves governing the Stokes phenomena for the solutions to the differential equation.

There is another point of view about the canonical quantization. The classical Seiberg-Witten curve arises here in the class-S construction of $N = 2$ pure SU(3) super Yang-Mills (SYM) theory. Geometrically, the canonical choice of quantum Seiberg-Witten curve should come from analyzing the conformal limit [19] of the Hitchin section [55] in the corresponding Hitchin moduli space. Such limit for the case of SL(N)-opers on a Riemann surface without any punctures has been analyzed in [68]. The conformal limit of Hitchin section for the case of punctured Riemann surfaces is in general not well-understood, even more so in the presence of irregular punctures.[8] Our strategy here will be experimental, we will give two possible quantization choices in (1.12) where both choices are motivated from [68]. As we will see, asymptotic analysis for spectral coordinates confirms both choices in (1.12) are valid quantizations for the classical class-S Seiberg-Witten curve of the pure SU(3) SYM. However, only one choice is *canonical* from the gauge theory point of view as we will derive in [47].

1.4 The SU3 equation

In this paper and its followup [47] we investigate the quantum Seiberg-Witten curve for the $N = 2$ pure SU(3) super Yang-Mills. Work exploring some perspectives of this theory has appeared in [61, 99, 101]. We start with the canonical Seiberg-Witten curve appearing in the class-S construction of $N = 2$ pure SU(3) SYM via compactifying a 6d $(2,0)$ theory of type A_2 on $\mathbb{CP}^1$ with two irregular singularities at $z = 0$ and $z = \infty$.

---

[8]For regular punctures, the canonical choice is the one under which the monodromies around regular punctures are unipotent.

We consider two possible quantizations of this Seiberg-Witten curve in terms of the following third-order differential equations:

$$
\begin{aligned}
A : & \quad \left[\partial_z^3 + \hbar^{-2}\frac{u_1}{z^2}\partial_z + \left(\hbar^{-3}\left(\frac{\Lambda}{z^4} + \frac{u_2}{z^3} + \frac{\Lambda}{z^2}\right) - \hbar^{-2}\frac{u_1}{z^3}\right)\right]\psi(z) = 0, \\
B : & \quad \left[\partial_z^3 + \hbar^{-2}\frac{u_1 + \hbar^2}{z^2}\partial_z + \left(\hbar^{-3}\left(\frac{\Lambda}{z^4} + \frac{u_2}{z^3} + \frac{\Lambda}{z^2}\right) - \hbar^{-2}\frac{u_1 + \hbar^2}{z^3}\right)\right]\psi(z) = 0,
\end{aligned}
\tag{1.12}
$$

where u_1 and u_2 are Coulomb branch parameters. We denote both equations as the SU(3) equations, they both produce Voros symbols with the expected asymptotics. However, equation B is the canonical quantum Seiberg-Witten curve from the gauge theory perspective as we describe more in [47]. In particular, the quantum periods for equation B obtained from using the abelianization method or the gauge theory perspective match with each other in relatively good precision.

As discussed in section 1.2, there are different methods to compute properly resummed quantum periods in this theory. In this paper we focus on the method described in section 1.2.1, namely we compute the Borel resummed quantum periods via abelianization. In the followup [47], we investigate the TBA method described in section 1.2.2 and the instanton calculus method described in section 1.2.3, along with perspectives from the instanton partition function of the $N = 2$ SU(3) Yang-Mills with the insertion of a canonical 1/2-BPS codimension-two surface defect.

Concretely, we study loci in both the strong-coupling region and the weak-coupling region. In the strong-coupling chamber with 12 BPS states, the Voros symbol $\mathcal{X}_\gamma(\hbar)$ could be expressed in terms of Wronskians of distinguished local solutions to (1.12) which decay exponentially as one goes into the irregular singularity at $z = 0$ or $z = \infty$. $\mathcal{X}_\gamma(\hbar)$ are certain coordinates for flat SL(3,$\mathbb{C}$)-connections over $\mathbb{CP}^1$ with two irregular singularities. We are not aware of a previous study of such coordinates. We also numerically evaluate $\log\left(\mathcal{X}_\gamma(\hbar)\right)$ and compare with the expected asymptotic quantum periods expansion truncated to a certain order in $\hbar$. We find good numerical agreement and view this as evidence that higher-order exact WKB analysis via abelianization does work as expected.

We also investigate certain loci in the weak-coupling region where $\mathcal{X}_\gamma(\hbar)$ is expressed using the exponentially decaying local solutions as one goes into an irregular singularity, as well as the eigenvectors of the monodromy around the irregular singularity. The $\mathcal{X}_\gamma(\hbar)$ constructed in such loci of the weak-coupling region is an instance of the higher length-twist coordinates. Different from examples in [46, 58], here $\mathcal{X}_\gamma(\hbar)$ are coordinates on a moduli space of flat SL(3,$\mathbb{C}$)-connections over a surface containing irregular singularities. We perform numerical checks against the expected asymptotic quantum periods expansion. Additionally, we comment on the exact quantization condition (EQC) for a bound state problem associated with the differential equation (1.12).

Finally we remark that it would be very interesting to have a gauge-theoretical derivation of the higher length-twist coordinates in this example and understand the generalized NRS conjecture by studying the canonical surface defect in the $N = 2$ pure SU(3) theory, following the work of [46].

2 Exact WKB and abelianization for SL(3)-opers

The exact WKB method is an approach to study the Stokes data of linear scalar differential equations. Originating from the study of Schrödinger equations, it has been developed in large number of studies, for a sampling of literature see e.g. [74, 102–106]. Recently the exact WKB method for higher order Schrödinger-like equations has also been initiated in [107–111].

In [31, 69] a new geometric reformulation of exact WKB has been proposed for Schrödinger operators and higher order opers. A key ingredient in this reformulation is a process of *abelianization*, which maps a flat SL(N,ℂ)-connection over a Riemann surface C to a flat GL(1,ℂ)-connection over a N-fold covering $\widetilde{C} \to C$. In this section we review exact WKB analysis in the language of abelianization, following closely the descriptions in [31].

Concretely, we focus on the case of SL(3)-opers, namely an third-order differential equation involving two meromorphic potentials $P_2(z, \hbar)$ and $P_3(z, \hbar)$:

$$\left[\partial_z^3 + \hbar^{-2} P_2(z, \hbar) \partial_z + \left(\hbar^{-3} P_3(z, \hbar) + \frac{1}{2} \hbar^{-2} P_2'(z, \hbar) \right) \right] \psi(z) = 0. \tag{2.1}$$

Although this equation is written explicitly in a single coordinate patch, it could be formulated on a Riemann surface C with a complex projective structure. In that context $\psi(z)$ is interpreted as a section of K_C^{-1} where K_C is the canonical bundle, P_2 is a meromorphic quadratic differential, and P_3 is a meromorphic cubic differential. In particular, equation (2.1) could be viewed as the quantization of the following Seiberg-Witten curve:

$$\widetilde{C} = \{ \lambda : \lambda^3 + p_2 \lambda + p_3 = 0 \} \subset T^* C, \tag{2.2}$$

where λ denotes the Seiberg-Witten differential, $p_{2,3}$ are the order-$\hbar^0$ terms in $P_{2,3}$.

The exact WKB method for SL(3)-opers (or higher SL(N)-opers) is not yet on solid footing in mathematics, however it was conjectured in [31] that the traditional exact WKB method for Schrödinger equations could be extended to SL(3)-opers by combining the methods developed in [69] with the scaling limit of [19]. Numerical evidence supporting this conjectural picture in certain examples have appeared in [31, 58, 67]. Our description here also builds upon this conjecture and we will provide further numerical evidence supporting this conjecture in sections 3 and 4.

2.1 The WKB solutions

The exact WKB method is centered around the construction of distinguished local WKB solutions, see e.g. [102, 104, 106] for the case of Schrödinger equations.

Written in local coordinate z on a contractible open set $U \subset C$, a WKB solution of (2.1) on U takes the following form:

$$\psi(z) = \exp\left(\frac{1}{\hbar} \int_{z_0}^z \lambda(z) dz \right), \tag{2.3}$$
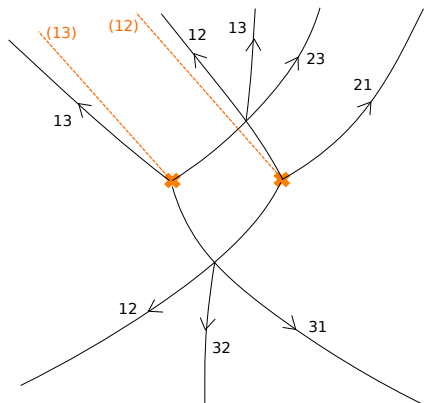
Figure 1. A representative local picture of a Stokes graph in the neighborhood of two simple branch points of different types. The orange crosses represent simple branch points, while the orange dashed lines represent the choice of branch cuts.

where $z_0 \in U$ is a chosen basepoint. For $\psi(z)$ to be a solution of (2.1), $\lambda(z)$ must obey the following third-order analogue of the Riccati equation:

$$\lambda^3(z) + 3\hbar\lambda(z)\partial_z\lambda(z) + \hbar^2\partial_z^2\lambda(z) + P_2(z,\hbar)\lambda(z) + P_3(z,\hbar) + \frac{1}{2}\hbar P_2'(z,\hbar) = 0. \qquad (2.4)$$

We first build a formal series solution λ^{formal} in powers of $\hbar$. At order-$\hbar^0$, the Riccati equation (2.4) becomes

$$\left(\lambda^{(0)}\right)^3 + p_2\lambda^{(0)} + p_3 = 0, \qquad (2.5)$$

where $\lambda^{(0)}$ is the leading order-$\hbar^0$ term in the formal series. Thus we encounter a 3-fold ambiguity, this could be resolved by choosing a solution to (2.5) or equivalently by choosing a sheet i of the following 3-fold covering of C:

$$\widetilde{C} = \{\lambda^{(0)} : \left(\lambda^{(0)}\right)^3 + p_2\lambda^{(0)} + p_3 = 0\}. \qquad (2.6)$$

In WKB language this is usually called the *WKB curve*, which could be identified with the Seiberg-Witten curve of a 4d $\mathcal{N} = 2$ theory. In particular, $\lambda^{(0)}$ corresponds to the Seiberg-Witten differential.

Once we have chosen a sheet i and the corresponding solution $\lambda_i^{(0)}$ to (2.5), higher order terms in the formal series are determined by solving (2.4) perturbatively in $\hbar$. For example, suppose we take $P_2 = 0$ and P_3 doesn't depend on $\hbar$, then the first few orders in this formal series take the form

$$\begin{aligned}
\lambda_i^{\text{formal}} &= \sum_{n=0}^{\infty} \lambda_i^{(n)}\hbar^n \\
&= \lambda_i^{(0)} - \hbar\frac{P_3'}{3P_3} + \hbar^2\frac{6P_3P_3'' - 7\left(P_3'\right)^2}{27P_3^2\lambda_i^{(0)}} + \dots
\end{aligned} \qquad (2.7)$$

By construction $\lambda_i^{\text{formal}}$ is only a formal series in $\hbar$, substituting $\lambda_i^{\text{formal}}$ into the WKB ansatz (2.3) we obtain formal solutions ψ_i^{formal} to the differential equation (2.1). A meaningful question is: under what conditions could one interpret ψ_i^{formal} as an asymptotic series

of certain actual solution ψ_i, such that $\psi_i \sim \psi_i^{\text{formal}}$ as $\hbar \to 0$? A natural way to produce the solutions ψ_i is to perform Borel resummation of ψ_i^{formal}. However, in general one can not do so *globally* on C, but only away from the so-called *Stokes curves.* The Stokes curves are one-dimensional curves on the Riemann surface C which divide C into different regions. Within each region Borel resummation produces actual solutions ψ_i, which jump as one goes across a Stokes curve.

In fact one can define Stokes curves more generally as θ-*Stokes curves* labeled by a phase θ. The conjectural picture is that away from such curves there exist actual solutions ψ_i^θ, such that ψ_i^θ has the desired expansion $\psi_i^\theta \sim \psi_i^{\text{formal}}$ as $\hbar \to 0$ while staying within the following half-plane

$$\mathbb{H}_\theta = \{\hbar : \operatorname{Re}\left(e^{-i\theta}\hbar\right) > 0\}. \tag{2.8}$$

Taking $\theta = \operatorname{Arg}(\hbar)$, one then obtains the Stokes curves appearing in the Borel resummation story.

The θ-Stokes curves are one-dimensional curves on the Riemann surface C carrying labels ij. They are defined as follows: along an oriented θ-Stokes curve of type ij, $e^{-i\theta}\left(\lambda_i^{(0)} - \lambda_j^{(0)}\right)dz$ is real and positive, where $\lambda_{i(j)}^{(0)}$ are the $i(j)$-th solution to the WKB curve (2.5). We remark that the above condition could be interpreted as the BPS conditions for solitons associated with the canonical surface defect in the corresponding class-S theory [69]. In this sense, the BPS soliton spectrum controls the Stokes phenomena for solutions to the quantum Seiberg-Witten curve, such as equation (2.1).

For simplicity suppose the 3-fold covering $\widetilde{C}$ only has simple branch points, then from each branch point there emanate three θ-Stokes curves. An important new feature of θ-Stokes curves for higher order SL(N)-opers is that a θ-Stokes curve of type ik could be born from the intersection of θ-Stokes curves of types ij and jk [69, 107, 108]. The collection of θ-Stokes curves defines the *Stokes graph W* at phase θ. Examples of Stokes graphs for the SU(3) equation could be found in figure 3, figure 4 and figure 5. In figure 1 we give a representative local picture of a Stokes graph in the neighborhood of two simple branch points.

Within a domain that doesn't contain any θ-Stokes curves of type ij, one obtains the actual solutions $\psi_i^\theta(z)$ and $\psi_j^\theta(z)$ to the SL(3)-oper equation (2.1). In particular, if the domain doesn't contain any θ-Stokes curves of any type we would obtain three solutions $\psi_{1,2,3}^\theta(z)$ which give a basis of solutions to the SL(3)-oper equation (2.1). As one crosses a θ-Stokes curve of type ij, the solution ψ_i^θ jumps by a constant multiple of ψ_j^θ. The rules for gluing together solutions across θ-Stokes curves could be formulated in the context of *abelianization* [69, 77], which we describe below.

2.2 Abelianization

The SL(3)-oper equation (2.1) could be written as a first order differential equation with 3×3 matrix coefficients. Concretely, in a local patch the equation is given as

$$\left[\partial_z + \hbar^{-1}\begin{pmatrix} 0 & -\frac{\sqrt{2}}{4}P_2 & \frac{P_3}{2} \\ \sqrt{2} & 0 & -\frac{\sqrt{2}}{4}P_2 \\ 0 & \sqrt{2} & 0 \end{pmatrix}\right]\begin{pmatrix} \frac{\hbar^3}{2}\psi''(z) + \frac{\hbar}{4}P_2\psi(z) \\ -\frac{\hbar^2}{\sqrt{2}}\psi'(z) \\ \hbar\psi(z) \end{pmatrix} = 0. \tag{2.9}$$

The SL(3)-oper equation can therefore be interpreted as a flat SL(3,$\mathbb{C}$)-connection ∇ in a jet bundle over C.

On the other hand, the WKB ansatz (2.3) could be interpreted as a solution to the following first-order differential equation

$$\left(\partial_z - \hbar^{-1}\lambda_i^\theta(z)\right)\psi_i^\theta(z) = 0. \tag{2.10}$$

This is equivalent to say that $\psi_i^\theta(z)$ corresponds to a flat section of an abelian GL(1,$\mathbb{C}$)-connection $\nabla^{\mathrm{ab},\theta}$ in a line bundle $\mathcal{L}$ over the Seiberg-Witten curve $\widetilde{C}$, where i labels the sheet index of the covering $\widetilde{C} \to C$. As described in [77], $\nabla^{\mathrm{ab},\theta}$ has monodromy -1 around branch points of $\widetilde{C} \to C$. Therefore, strictly speaking, $\nabla^{\mathrm{ab},\theta}$ is an *almost-flat* connection over $\widetilde{C}$.

From this point of view, finding WKB solutions $\psi_i^\theta(z)$ to the SL(3)-oper equation (2.1) could be reformulated as finding the map from a flat SL(3,$\mathbb{C}$)-connections ∇ over C to an almost-flat GL(1,$\mathbb{C}$)-connection $\nabla^{\mathrm{ab},\theta}$ over $\widetilde{C}$, using the Stokes graph W at phase θ. Such procedure is denoted as the W-abelianization of ∇ and has been studied in [69, 77, 79]. For a given ∇ and a given Stokes graph W, there are finitely many W-abelianizations of ∇. For the choice of $\theta = \arg(\hbar)$, exact WKB analysis selects a distinguished W-abelianization of ∇ [112].

Concretely, the W-abelianization procedure provides a gluing formula for local solutions across θ-Stokes curves. Recall that in the complement of the θ-Stokes graph, we have bases of local solutions ψ_i^θ to the SL(3)-oper equation (2.1), however such solutions could be different on the two sides of a θ-Stokes curve. One can nevertheless give a gluing map which takes solutions on the left hand side of a θ-Stokes curve to solutions on the right hand side. Across a θ-Stokes curve of type ij, the gluing prescription could be summarized as

$$\begin{pmatrix}\psi_i^L \\ \psi_j^L \\ \psi_k^L\end{pmatrix} \mapsto \begin{pmatrix}1 & x & 0 \\ 0 & 1 & 0 \\ 0 & 0 & 1\end{pmatrix}\begin{pmatrix}\psi_i^L \\ \psi_j^L \\ \psi_k^L\end{pmatrix} = \begin{pmatrix}\frac{[\psi_i^L,\psi_j^L,\psi_k^L]}{[\psi_i^R,\psi_j^L,\psi_k^L]}\psi_i^R \\ \frac{[\psi_j^L,\psi_k^L,\psi_i^L]}{[\psi_j^R,\psi_k^L,\psi_i^L]}\psi_j^R \\ \frac{[\psi_k^L,\psi_i^L,\psi_j^L]}{[\psi_k^R,\psi_i^L,\psi_j^L]}\psi_k^R\end{pmatrix}, \tag{2.11}$$

where x is certain constant, and $[\psi_i,\psi_j,\psi_k]$ denotes the Wronskian of the three solutions.

As we will see in sections 3 and 4, for special values of θ it could happen that a θ-Stokes curve of type ij coincides with a θ-Stokes curve of type ji. In this case, the gluing prescription is chosen to be[9]

$$\begin{pmatrix}\psi_i^L \\ \psi_j^L \\ \psi_k^L\end{pmatrix} \mapsto \begin{pmatrix}z & x & 0 \\ y & z & 0 \\ 0 & 0 & 1\end{pmatrix}\begin{pmatrix}\psi_i^L \\ \psi_j^L \\ \psi_k^L\end{pmatrix} = \begin{pmatrix}\sqrt{\frac{[\psi_i^L,\psi_j^L,\psi_k^L][\psi_i^L,\psi_j^R,\psi_k^L]}{[\psi_i^R,\psi_j^R,\psi_k^L][\psi_i^R,\psi_j^L,\psi_k^L]}}\psi_i^R \\ \sqrt{\frac{[\psi_j^L,\psi_i^L,\psi_k^L][\psi_j^L,\psi_i^R,\psi_k^L]}{[\psi_j^R,\psi_i^R,\psi_k^L][\psi_j^R,\psi_i^L,\psi_k^L]}}\psi_j^R \\ \frac{[\psi_k^L,\psi_i^L,\psi_j^L]}{[\psi_k^R,\psi_i^L,\psi_j^L]}\psi_k^R\end{pmatrix}, \tag{2.12}$$

where $z^2 - xy = 1$.

---

[9]As described in [31], there are other possible choices for the gluing formula. The one we use here amounts to an "averaged" choice.

2.3 The spectral coordinates

The spectral coordinates are defined as holonomies of the almost-flat GL(1,$\mathbb{C}$)-connection $\nabla^{\mathrm{ab},\theta}$ along 1-cycles γ on $\widetilde{C}$:

$$\mathcal{X}_\gamma^\theta = \mathrm{Hol}_\gamma \nabla^{\mathrm{ab},\theta} \in \mathbb{C}^\times, \quad \gamma \in H_1(\widetilde{C}, \mathbb{Z}). \tag{2.13}$$

By applying the gluing formulae (2.11) and (2.12), $\mathcal{X}_\gamma^\theta$ can be expressed in terms of the Wronskians of local solutions $\psi_i^\theta(z)$ to the SL(3)-oper equation (2.1). For the SU(3) equation (1.12) considered in this article, as we will see in sections 3 and 4, the gluing prescriptions impose relations among local solutions $\psi_i^\theta(z)$ in different regions separated by θ-Stokes curves. After solving such constraints the $\mathcal{X}_\gamma^\theta$ are expressed in terms of Wronskians of distinguished local solutions, either as asymptotically decaying solutions as z approaches a singularity or as eigenvectors of the monodromy around a loop. In this way, $\mathcal{X}_\gamma^\theta$ are identified with certain coordinate functions on a moduli space of flat SL(3,$\mathbb{C}$)-connections. In particular, for certain special loci in the weak-coupling region, as will be described in section 4, we obtain coordinates of higher length-twist type generalizing complexified Fenchel-Nielsen coordinates [18, 113]. Higher length-twist coordinates have also been studied in other examples in [46, 58].

The spectral coordinates depend on the following quantities: the phase θ, Planck's constant $\hbar$, and the potentials P_2 and P_3 encoding Coulomb branch parameters etc. As long as the topology of θ-Stokes graph doesn't change, the dependence on θ is trivial. However, in the (P_2, P_3, θ) parameter space there is a codimension-1 locus where the topology of θ-Stokes graph changes [53, 69]. Such locus corresponds to the existence of 4d BPS states and is often denoted as the BPS locus. Across the BPS locus, $\mathcal{X}_\gamma^\theta$ jump by the Kontsevich-Soibelman transformation [53, 69, 83].

The spectral coordinates have nice asymptotic properties: as $\hbar \to 0$ in the half plane $\mathbb{H}_\theta$ defined in (2.8), $\mathcal{X}_\gamma^\theta$ is expected to admit the following asymptotic expansion [31]:

$$\mathcal{X}_\gamma^\theta \sim \exp\left[\frac{1}{\hbar} \oint_\gamma \lambda^{\mathrm{formal}} dz\right]. \tag{2.14}$$

If $\hbar$ is exactly located on the center ray of $\mathbb{H}_\theta$, or equivalently $\theta = \arg(\hbar)$, then $\mathcal{X}_\gamma^{\arg(\hbar)}$ have stronger properties [31]. If (P_2, P_3, θ) is not on the BPS locus, $\mathcal{X}_\gamma^{\arg(\hbar)}$ is conjectured to be the Borel summation of the asymptotic expansion (2.14). If (P_2, P_3, θ) happens to be on the BPS locus, then the corresponding Borel transform might have singularities[10] and the asymptotic series might not be Borel summable in which case $\mathcal{X}_\gamma^{\arg(\hbar)}$ is expected to produce the median Borel summation from (2.14). In summary, asymptotic properties of the spectral coordinates enables one to compute Borel resummed quantum periods series (1.8) using abelianization methods.

---

[10]This happens if γ has non-trivial DSZ pairing with the IR charge of the 4d BPS state appearing at the BPS locus.
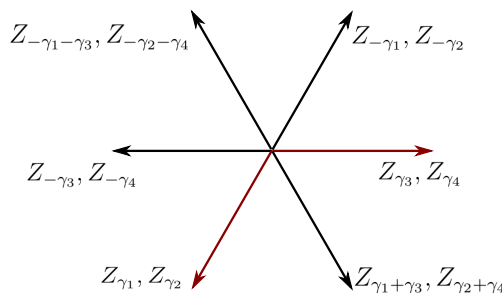
Figure 2. Central charges of the 12 BPS states at $u_1 = u_2 = 0$.

3 The SU(3) equation in the strong-coupling region

From now on, we specialize to the SU(3) equations (1.12), which corresponds to the quantum Seiberg-Witten curve for 4d $N = 2$ pure SU(3) SYM. In this section we focus on the analysis in the strong-coupling region, while in section 4 we study (1.12) in the weak-coupling region.

3.1 The BPS spectrum

In the strong-coupling region, u_1 and u_2 are small and the BPS spectrum is finite, consisting of 12 BPS states [69, 114–116]. We choose a positive basis $\{\gamma_1, \gamma_2, \gamma_3, \gamma_4\}$ for the IR electromagnetic charge lattice. Geometrically, γ_i corresponds to homology classes in $H_1(\widetilde{C}, \mathbb{Z})$ where $\widetilde{C}$ is the Seiberg-Witten curve. We show representative cycles in these holomogy classes in figure 4. Identifying the Dirac-Schwinger-Zwanziger pairing with the intersection pairing in $H_1(\widetilde{C}, \mathbb{Z})$, we obtain the following pairing matrix with respect to the chosen basis $\{\gamma_1, \gamma_2, \gamma_3, \gamma_4\}$:

$$\begin{pmatrix} 0 & 0 & 1 & -2 \\ 0 & 0 & -2 & 1 \\ -1 & 2 & 0 & 0 \\ 2 & -1 & 0 & 0 \end{pmatrix}. \tag{3.1}$$

The 12 BPS states have the following IR charges:

$$\pm \gamma_1, \pm\gamma_2, \pm\gamma_3, \pm\gamma_4, \pm(\gamma_1 + \gamma_3), \pm(\gamma_2 + \gamma_4). \tag{3.2}$$

The BPS spectrum respects a $\mathbb{Z}_6$ symmetry induced by the action of the discrete R-symmetry on the central charge operator. In particular, if we take $u_1 = u_2 = 0$ the BPS states have phases $0, \pi/3, 2\pi/3, \pi, 4\pi/3, 5\pi/3$ and their central charges have the same norm. This is illustrated in figure 2.

3.2 Stokes graphs

As described in section 2, the Stokes graph appearing in the exact WKB method depends on a phase parameter θ. In particular, if θ happens to be a phase equal to the central charge phase of a 4d BPS hypermultiplet the corresponding Stokes graph contains finite segments or webs. If θ happens to be equal to the phase of a 4d BPS vector multiplet,
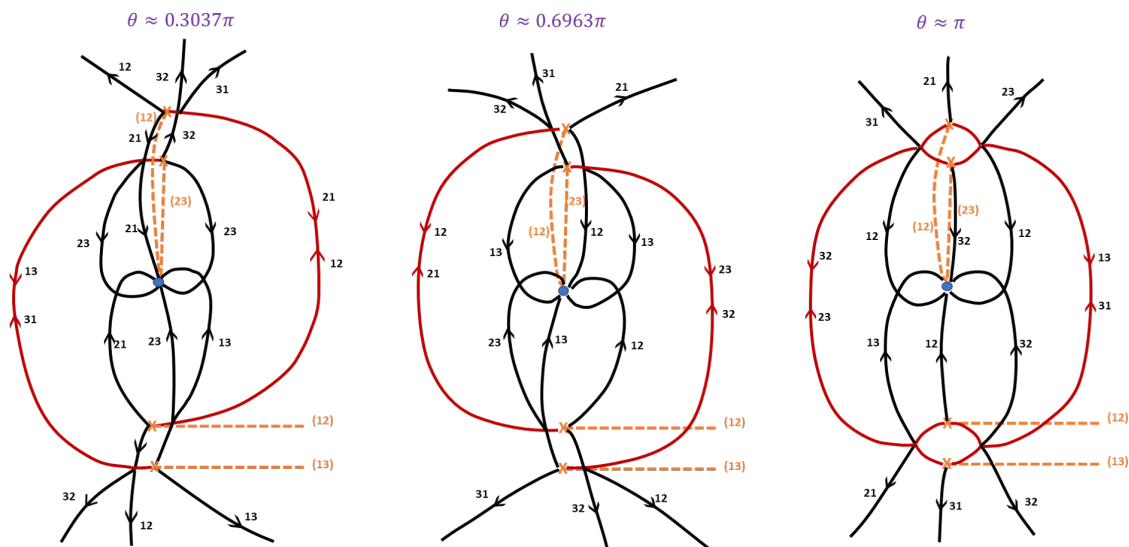
Figure 3. Zoomed-in Stokes graphs at $\theta \approx 0.3037\pi, 0.6963\pi, \pi$, where we have taken $u_1 = 0.3$, $u_2 = 0, \Lambda = 1$ and we focus on details near $z = 0$. The irregular singularity at $z = 0$ is denoted by a blue dot. The irregular singularity at $z = \infty$ is not shown in the figure. Branch points are represented as orange crosses, while orange dashed lines denote the choice of branch cuts. Finite segments or webs are colored in red. In the class S setup [52, 53, 69] they correspond to the trajectories of 6d BPS strings which give rise to 4d BPS states after the twisted compactification on C.

the Stokes graph would contain annulus domain. Such phases are usually called *critical phases*. For example, taking $u_1 = 0.3$, $u_2 = 0$ and $\Lambda = 1$, in figure 3 we show the Stokes graphs zoomed in around $z = 0$ at critical phases $\theta \approx (0.3037\pi, 0.6963\pi, \pi)$.[11] Details of the Stokes graphs at large $|z|$ are similar to what is shown in figure 4.

At the special point $u_1 = u_2 = 0$, Stokes graphs at critical phases all look the same except that the sheet labeling gets permuted. As an example, figure 4 shows the Stokes graph at $\theta = \pi/3$. In the following, we will derive an expression for the spectral coordinates in terms of the distinguished local solutions to the SU(3) equation (1.12).

3.3 Solving the abelianization problem

The Stokes graph in figure 4 divides the punctured-plane into 16 regions; in each region we could choose a basis of local WKB solutions to the SU(3) equation (1.12). In particular, there are two distinguished local solutions:

- The local WKB solution t near $z = 0$ characterized as a solution which decays exponentially as $z \to 0$ along the negative imaginary axis.

- The local WKB solution s near $z = \infty$ characterized as a solution which decays exponentially as $z \to \infty$ along the negative imaginary axis.

---

[11]The Stokes graph at phase $\theta + \pi$ looks almost identical to that at phase θ, except the arrow directions are reversed. Therefore it suffices to consider Stokes graphs at phases within $(0, \pi]$.
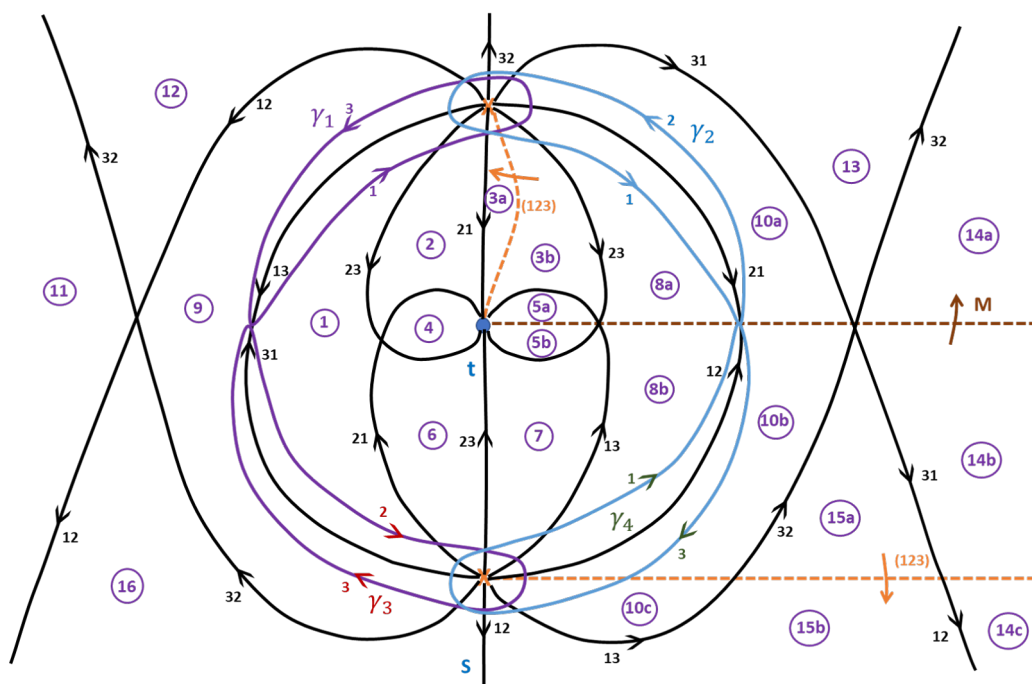
Figure 4. The Stokes graph at $\theta = \pi/3$ with $u_1 = u_2 = 0$ and $\Lambda = 1$. The irregular singularity at $z = 0$ is represented by a blue dot, while the irregular singularity at $z = \infty$ is not shown in the figure. Branch points and branch cuts are denoted by orange crosses and orange dashed lines respectively. The monodromy cut is represented by a brown dotted line. We also show representative cycles corresponding to the basis charges γ_1, γ_2, γ_3 and γ_4 in purple, blue, red and green respectively. The Stokes graph divides the punctured-plane into 16 regions, which are labeled by circled purple numbers.

Based on the gluing rules in section 2.2, we could immediately identify a few local WKB solutions in some regions in figure 4 as s, t or their images under the monodromy actions M and M^{-1} around the irregular singularity. However, across the 16 regions there are 10 local WKB solutions which are not straightforwardly related to the distinguished ones which we denote as ψ_i $(i = 1, \ldots, 10)$. The local WKB solutions in the 16 regions are listed in table 1. Here to write the basis concretely as an ordered tuple we have used the trivialization of $\widetilde{C}$ away from the branch cuts.

The concrete task of abelianization is solving ψ_i in terms of distinguished local solutions and the monodromy M. For this purpose, we consider constraints coming from gluing factors across θ-Stokes curves. As an example, the gluing factor across the θ-Stokes curve of type 13 between regions $3b$ and $5a$ indicates that ψ_2, Mt, M^2t are co-planar in the solution space. Let us denote $\langle \alpha, \beta \rangle$ as the two-dimensional plane spanned by α and β in the three-dimensional space of local solutions, then we have $\langle \psi_2, Mt \rangle = \langle M^2t, Mt \rangle$. Similarly, the gluing factor across the coincident θ-Stokes curves of type 12 and 21 between regions $8a$ and $10a$ implies $\langle \psi_2, M\psi_5 \rangle = \langle Ms, s \rangle$. For generic M, ψ_2 then corresponds to the intersection between $\langle Ms, s \rangle$ and $\langle M^2t, Mt \rangle$. All of the 10 local WKB solutions ψ_i

region	basis	region	basis
1	(Mt, s, t)	2	(Mt, ψ_1, t)
3a	(Mt, ψ_2, t)	3b	(ψ_2, t, Mt)
4	(Mt, ψ_3, t)	5a	(M^2t, t, Mt)
5b	$(Mt, M^{-1}t, t)$	6	(Mt, ψ_4, t)
7	(Mt, ψ_5, t)	8a	$(\psi_2, M\psi_5, Mt)$
8b	$(M^{-1}\psi_2, \psi_5, t)$	9	(ψ_6, s, ψ_7)
10a	(Ms, s, Mt)	10b	$(s, M^{-1}s, t)$
10c	$(t, s, M^{-1}s)$	11	$(Ms, s, M^{-1}s)$
12	(Ms, s, ψ_7)	13	(Ms, s, ψ_8)
14a	(Ms, s, ψ_9)	14b	$(s, M^{-1}s, M^{-1}\psi_9)$
14c	$(M^{-1}\psi_9, s, M^{-1}s)$	15a	$(s, M^{-1}s, \psi_{10})$
15b	$(\psi_{10}, s, M^{-1}s)$	16	$(\psi_6, s, M^{-1}s)$

Table 1. Bases of local WKB solutions for the 16 regions shown in figure 4.

could be determined in a similar fashion:

$$
\begin{aligned}
\psi_1 &= \langle s, t \rangle \cap \langle M^2 t, Mt \rangle, & \psi_2 &= \langle Ms, s \rangle \cap \langle M^2 t, Mt \rangle, \\
\psi_3 &= \langle M^2 t, Mt \rangle \cap \langle M^{-1} t, t \rangle, & \psi_4 &= \langle Mt, s \rangle \cap \langle M^{-1} t, t \rangle, \\
\psi_5 &= \langle s, M^{-1} s \rangle \cap \langle M^{-1} t, t \rangle, & \psi_6 &= \langle Ms, s \rangle \cap \langle Mt, t \rangle, \\
\psi_7 &= \langle M^{-1} s, s \rangle \cap \langle Mt, t \rangle, & \psi_8 &= \langle M^{-1} s, s \rangle \cap \langle Mt, Ms \rangle, \\
\psi_9 &= \langle M^{-1} s, s \rangle \cap \langle M^2 s, Ms \rangle, & \psi_{10} &= \langle t, M^{-1} s \rangle \cap \langle Ms, s \rangle.
\end{aligned}
\tag{3.3}
$$

3.4 The spectral coordinates

Let $\mathcal{X}_{\gamma_i}$,[12] denote the holonomy of $\nabla^{\mathrm{ab},\theta}$ along cycles γ_i shown in figure 4. The $\mathcal{X}_{\gamma_i}$ are then certain spectral coordinates for the flat SL(3,$\mathbb{C}$)-connection ∇. We remark that, although the Stokes graph in figure 4 was drawn at the special point $u_1 = u_2 = 0$, the expressions for $\mathcal{X}_{\gamma_i}$ in terms of distinguished local solutions hold as we move to small non-zero $u_{1,2}$. The Stokes graph doesn't go through topological changes in that process.

Applying the gluing formulae (2.11) and (2.12), these spectral coordinates are given in terms of the Wronskians of distinguished local solutions:

$$
\begin{aligned}
\mathcal{X}_{\gamma_1} &= \frac{[Mt, Ms, s][\psi_7, \psi_6, s][t, M^{-1}s, s]}{[\psi_7, s, Ms][t, Mt, s][\psi_6, s, M^{-1}s]}, \\
\mathcal{X}_{\gamma_2} &= \frac{[s, t, Mt][M^{-1}\psi_2, \psi_5, t][s, Mt, t]}{[M^{-1}\psi_2, t, M^{-1}t][Ms, s, Mt][\psi_5, t, Mt]}, \\
\mathcal{X}_{\gamma_3} &= \frac{[\psi_5, s, t][M^{-1}s, s, \psi_6][M^{-1}t, t, M^{-1}\psi_2]}{[\psi_5, t, Mt][M^{-1}s, s, t][M^{-1}s, M^{-1}\psi_2, t]} \sqrt{\frac{[s, Mt, t][\psi_7, Mt, s]}{[\psi_7, s, \psi_6][t, \psi_6, s]}}, \\
\mathcal{X}_{\gamma_4} &= \frac{[\psi_6, t, s][Mt, t, \psi_5], [Ms, s, \psi_7]}{[\psi_6, s, M^{-1}s][Mt, t, s][Mt, \psi_7, s]} \sqrt{\frac{[t, M^{-1}s, s][M^{-1}\psi_2, M^{-1}s, t]}{[M^{-1}\psi_2, t, \psi_5][s, \psi_5, t]}},
\end{aligned}
\tag{3.4}
$$

---

[12]From now on, we suppress the dependence on θ in the notation for spectral coordinates for compactness reasons.

	$\hbar = e^{i\pi/3}$		$\hbar = \frac{1}{2}e^{i\pi/3}$	
	evaluation of (3.4)	$\frac{1}{\hbar}\Pi_\gamma(\hbar)$ at $o(\hbar^6)$	evaluation of (3.4)	$\frac{1}{\hbar}\Pi_\gamma(\hbar)$ at $o(\hbar^6)$
$\log\mathcal{X}_{\gamma_1}$	-3.5756	-3.5873	-10.2481	-10.2482
$\log\mathcal{X}_{\gamma_2}$	-3.5756	-3.5873	-10.2481	-10.2482
$\log\mathcal{X}_{\gamma_3}$	$1.7878 - 0.4490i$	$1.7937 - 0.4405i$	$5.12405 + 1.88253i$	$5.12412 + 1.88266i$
$\log\mathcal{X}_{\gamma_4}$	$1.7878 - 0.4490i$	$1.7937 - 0.4405i$	$5.12405 + 1.88253i$	$5.12412 + 1.88266i$

Table 2. Comparison of $\log\mathcal{X}_\gamma$ with the formal quantum periods expansion up to order-$\hbar^6$ at $\hbar = e^{i\pi/3}$ and $\hbar = \frac{1}{2}e^{i\pi/3}$ for equation A of (1.12), where we have set $u_1 = u_2 = 0$ and $\Lambda = 1$.

where $\psi_{2,5,6,7}$ are intersections of certain planes spanned by the distinguished local solutions s, t and their images under the monodromy action. They are given explicitly in (3.3).

As a remark, the expressions for $\mathcal{X}_{\gamma_i}$ in (3.4) correspond to the critical Stokes graph (figure 4) at $\theta = \pi/3$. Following the same procedure as described above, we also obtain expressions for the spectral coordinates $\mathcal{X}_{\gamma_i}^\pm$ at $\theta = \pi/3 + \epsilon$ and $\theta = \pi/3 - \epsilon$ for small ϵ. $\mathcal{X}_{\gamma_1}^\pm$ and $\mathcal{X}_{\gamma_2}^\pm$ have the same expression as in (3.4). Meanwhile $\mathcal{X}_{\gamma_3}^+$ ($\mathcal{X}_{\gamma_4}^+$) differs from $\mathcal{X}_{\gamma_3}^-$ ($\mathcal{X}_{\gamma_4}^-$) by a Kontsevich-Soibelman transformation involving $\mathcal{X}_{\gamma_{1,2}}$. The $\mathcal{X}_{\gamma_{3,4}}$ in (3.4) could be thought of as an average of $\mathcal{X}_{\gamma_{3,4}}^\pm$. These properties are consistent with the expected Stokes phenomena for the Borel-resummed quantum periods, which are controlled by the BPS spectrum illustrated in figure 2. Concretely, across the phase $\theta = \pi/3$, spectral coordinates $\mathcal{X}_\gamma$ where γ has non-trivial DSZ pairing with $\gamma_{1,2}$ would jump by a Kontsevich-Soibelman transformation.

We further remark that the Wronskian expressions of $\mathcal{X}_\gamma$ in (3.4) are the same for both quantization choices in (1.12); this is because the Stokes graph is determined by the classical Seiberg-Witten curve as described in section 2.1. However, it is true that the concrete special solutions such as s and t differ between the two quantization choices resulting different numerical values of $\mathcal{X}_\gamma$.

3.5 The asymptotic behavior

As $\hbar \to 0$ while staying within the half-plane $\mathbb{H}_\theta$ defined in (2.8), $\hbar\log\mathcal{X}_\gamma$ is conjectured to have an asymptotic series expansion given by the formal quantum periods series (1.8). We perform numerical checks against this conjecture. On the one hand, we evaluate (3.4) by numerically solving (1.12) and computing the Wronskians of distinguished solutions. On the other hand, we can compute the truncated series in $\hbar$ of the formal quantum periods $\Pi_\gamma(\hbar)$. For example, we first consider the differential equation A in (1.12). Taking $u_1 = u_2 = 0$ and $\Lambda = 1$, numerical results for $\hbar = e^{i\pi/3}$ and $\hbar = \frac{1}{2}e^{i\pi/3}$ are listed in table 2.

From table 2 we see that as $|\hbar|$ gets smaller, the spectral coordinates obtained via the abelianization method get closer to the truncated quantum periods expansion.[13] This is in line with the conjectured asymptotic behavior of spectral coordinates. Unfortunately,

---

[13]As $\Pi_\gamma(\hbar)$ is an asymptotic series, there exist an optimal term where the agreement would be the best. Here we approximate the optimal term by numerical experiments.

	$\hbar = \frac{1}{2}e^{i\pi/3}$	
	evaluation of (3.4)	$\frac{1}{\hbar}\Pi_\gamma(\hbar)$ at $o(\hbar^6)$
$\log\mathcal{X}_{\gamma_1}$	-11.21119	-11.21120
$\log\mathcal{X}_{\gamma_2}$	-11.21119	-11.21120
$\log\mathcal{X}_{\gamma_3}$	$5.60559 + 2.71805i$	$5.60560 + 2.71808i$
$\log\mathcal{X}_{\gamma_4}$	$5.60559 + 2.71805i$	$5.60560 + 2.71808i$

Table 3. Comparison of $\log\mathcal{X}_\gamma$ with the formal quantum periods expansion up to order-$\hbar^6$ at $\hbar = \frac{1}{2}e^{i\pi/3}$ for equation B of (1.12), where we have set $u_1 = u_2 = 0$ and $\Lambda = 1$.

numerical evaluation of (3.4) becomes rather difficult for small $|\hbar|$; we are not able to demonstrate the asymptotic behavior at smaller $|\hbar|$. Nevertheless, we regard table 2 as the evidence that the higher-order exact WKB method indeed works. As a further remark, we notice that the system has a symmetry where $\mathcal{X}_{\gamma_1} = \mathcal{X}_{\gamma_2}$ and $\mathcal{X}_{\gamma_3} = \mathcal{X}_{\gamma_4}$. The numerical values in table 2 do respect such symmetry, which could serve as an extra consistency check for our analysis. We perform similar analysis for equation B of (1.12). Here the numerical agreement seems slightly better; we list the values at $\hbar = \frac{1}{2}e^{i\pi/3}$ in table 3. The asymptotic analysis suggests that both differential equations A and B of (1.12) are valid quantization choices of the classical Seiberg-Witten curve, although the differential equation B is the canonical quantization from the gauge theory point of view, as we will describe in upcoming [47].

4 The SU(3) equation in the weak-coupling region

4.1 A Stokes graph

Now we turn our attention to the weak-coupling region, where the BPS spectrum becomes very complicated [115]. In particular, we consider parameters under which a Stokes graph of the higher length-twist type [58] appears. Our motivation for considering such Stokes graphs is, as briefly described in section 1.2.3, to make connections with gauge theory calculations. The corresponding spectral coordinates are higher length-twist coordinates, which are closely related to the quantum a and a_D periods. In this paper we construct the higher length-twist coordinates using abelianization methods, while perspectives from instanton calculus is investigated in [47].

Taking $\Lambda = 1$, $u_2 = 0$, and real $u_1 > 1.25$, at $\theta = 0$ the Stokes graph looks like figure 5. In particular, we see a ring domain corresponding to the W-bosons; this ring domain is denoted as the region 7 in figure 5. We choose a basis $\{\gamma_1', \gamma_2', \gamma_3', \gamma_4'\}$ of the IR charge lattice as shown in figure 5. This basis is more natural for the analysis in the weak-coupling region. We will write down the corresponding spectral coordinates $\mathcal{X}_{\gamma_i'}$ in section 4.3. In particular, $\mathcal{X}_{\gamma_{1,2}'}$ are higher length coordinates and $\mathcal{X}_{\gamma_{3,4}'}$ are higher twist coordinates.
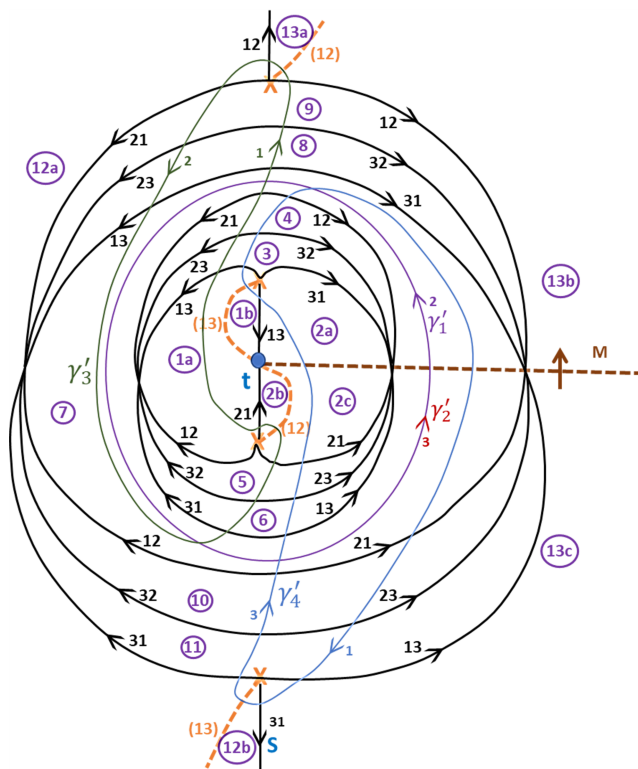
Figure 5. The Stokes graph at $\theta = 0$, with $u_1 = 4.5$, $u_2 = 0$ and $\Lambda = 1$. The notation conventions are the same as those in figure 4. We show representative cycles corresponding to the basis charges γ_1', γ_2', γ_3' and γ_4' in purple, red, green and blue respectively. This Stokes graph divides the punctured-plane into 13 regions.

4.2 Solving the abelianization problem

The Stokes graph in figure 5 divides the punctured-plane into 13 regions. The local WKB solutions in each region turn out to be expressed in terms of the following distinguished local solutions:

- The local WKB solution t near $z = 0$ and the local WKB solution s near $z = \infty$, characterized as exponentially decaying solution as $z \to 0$ and $z \to \infty$ respectively, along the negative imaginary axis.

- Eigenvectors α, β and γ of the counterclockwise monodromy M around $z = 0$. For the parameter range we consider here, namely real $u_1 > 1.25$, $u_2 = 0$ and $\hbar \in \mathbb{R}_+$, the eigenvalues of the monodromy M are all real and positive. Moreover, one of the eigenvalues is 1. Let us denote the eigenvalues of M as μ_α, μ_β and μ_γ, corresponding to the eigenvectors α, β and γ respectively. Then α, β and γ are specified according to the condition $\mu_\alpha = 1$, $\mu_\beta > 1$ and $\mu_\gamma < 1$.[14]

---

[14]One might wonder where this particular specification for α, β and γ comes from. After all, given a generic monodromy matrix M we have 6 ways of defining (α, β, γ). The choice we take here is the one which matches the leading asymptotic behavior of spectral coordinates given by the classical periods around the ring domain.

region	basis	region	basis
1a	$(t, Mt, M^{-1}t)$	1b	$(M^{-1}t, Mt, t)$
2a	$(M\phi_1, Mt, t)$	2b	$(t, \phi_1, M^{-1}t)$
2c	$(\phi_1, t, M^{-1}t)$	3	(ϕ_2, Mt, ϕ_3)
4	(ϕ_2, ϕ_4, γ)	5	$(\phi_5, \phi_6, M^{-1}t)$
6	(ϕ_5, β, ϕ_7)	7	(α, β, γ)
8	(ϕ_8, β, ϕ_9)	9	(ϕ_8, ϕ_{10}, s)
10	$(\phi_{11}, \phi_{12}, \gamma)$	11	$(\phi_{11}, Ms, \phi_{13})$
12a	(ϕ_{14}, Ms, s)	12b	(s, Ms, ϕ_{14})
13a	$(M^2 s, Ms, s)$	13b	$(Ms, M^2 s, s)$
13c	$(s, Ms, M^{-1}s)$		

Table 4. Bases of local WKB solutions for the 13 regions shown in figure 5.

We proceed by first listing bases of local WKB solutions for each region in table 4. In this case there are 14 local solutions ϕ_i not straightforwardly related to the above distinguished solutions and their images under the monodromy action.

Similar to the strong coupling case described in section 3.3, by exploring the constraints imposed by the gluing condition we could solve for ϕ_i. The solutions are given as follows:

$$
\begin{aligned}
\phi_1 &= \langle t, Mt \rangle \cap \langle M^{-2}t, M^{-1}t \rangle, & \phi_2 &= \langle t, M^{-1}t \rangle \cap \langle \alpha, \beta \rangle, \\
\phi_3 &= \langle t, M^{-1}t \rangle \cap \langle Mt, \gamma \rangle, & \phi_4 &= \langle Mt, \gamma \rangle \cap \langle \alpha, \beta \rangle, \\
\phi_5 &= \langle t, Mt \rangle \cap \langle \alpha, \gamma \rangle, & \phi_6 &= \langle t, Mt \rangle \cap \langle M^{-1}t, \beta \rangle, \\
\phi_7 &= \langle M^{-1}t, \beta \rangle \cap \langle \alpha, \gamma \rangle, & \phi_8 &= \langle \alpha, \gamma \rangle \cap \langle Ms, M^2 s \rangle, \\
\phi_9 &= \langle \alpha, \gamma \rangle \cap \langle \beta, s \rangle, & \phi_{10} &= \langle \beta, s \rangle \cap \langle Ms, M^2 s \rangle, \\
\phi_{11} &= \langle \alpha, \beta \rangle \cap \langle s, M^{-1}s \rangle, & \phi_{12} &= \langle \alpha, \beta \rangle \cap \langle Ms, \gamma \rangle, \\
\phi_{13} &= \langle Ms, \gamma \rangle \cap \langle s, M^{-1}s \rangle, & \phi_{14} &= \langle s, M^{-1}s \rangle \cap \langle M^2 s, Ms \rangle.
\end{aligned}
\tag{4.1}
$$

4.3 The spectral coordinates

The spectral coordinates $\mathcal{X}_{\gamma'_{1,2}}$ could be identified with the higher length coordinates on the moduli space of flat SL(3,$\mathbb{C}$)-connections. They are simply given by the corresponding eigenvalues of the monodromy action:

$$
\mathcal{X}_{\gamma'_1} = \mu_\beta, \quad \mathcal{X}_{\gamma'_2} = \mu_\gamma.
\tag{4.2}
$$

The spectral coordinates $\mathcal{X}_{\gamma'_{3,4}}$ are higher twist coordinates. We express them via Wronskians of the distinguished local solutions:

$$
\begin{aligned}
\mathcal{X}_{\gamma'_3} = &\sqrt{-\frac{[Ms, \phi_{14}, s][Ms, \phi_8, s][\phi_{10}, \phi_9, \phi_8][\beta, \phi_7, \phi_5][\beta, M^{-1}t, \phi_5][\phi_6, \phi_1, M^{-1}t][t, M^{-1}t, Mt]}{[\phi_{10}, \phi_{14}, s][\beta, \phi_9, \phi_8][\beta, s, \phi_8][\phi_6, \phi_7, \phi_5][t, \phi_1, M^{-1}t][t, \phi_5, M^{-1}t][\phi_2, \phi_3, Mt]}} \\
&\times \sqrt{\frac{[t, \phi_3, Mt][\phi_2, \phi_4, \gamma][\phi_2, \beta, \gamma][\alpha, \phi_9, \beta][\phi_8, \phi_{10}, s][\phi_8, M^2 s, s]}{[\phi_2, M^{-1}t, Mt][\alpha, \phi_4, \gamma][\phi_8, \phi_9, \beta][\phi_8, \gamma, \beta][Ms, M^2 s, s][Ms, \phi_{10}, s]}},
\end{aligned}
$$

$$\mathcal{X}_{\gamma_4'} = \frac{1}{\mu_\alpha} \sqrt{\frac{[s, \phi_{14}, Ms][s, \phi_{11}, Ms][\phi_{13}, \phi_{12}, \phi_{11}][\gamma, \alpha, \beta][\gamma, \phi_5, \beta][\phi_7, \phi_6, \phi_5][t, M^{-1}t, Mt]}{[\phi_{13}, \phi_{14}, Ms][\gamma, \phi_{12}, \phi_{11}][\gamma, Ms, \phi_{11}][\phi_7, \alpha, \beta][M^{-1}t, \phi_6, \phi_5][M^{-1}t, \beta, \phi_5][\phi_2, \phi_3, Mt]}}$$

$$\times \sqrt{\frac{[t, \phi_3, Mt][\phi_2, \phi_4, \gamma][\phi_2, \beta, \gamma][\alpha, \phi_{12}, \gamma][\phi_{11}, \phi_{13}, Ms][\phi_{11}, M^{-1}s, Ms]}{[\phi_2, M^{-1}t, Mt][\alpha, \phi_4, \gamma][\phi_{11}, \psi_{12}, \gamma][\phi_{11}, \beta, \gamma][s, M^{-1}s, Ms][s, \phi_{13}, Ms]}}, \tag{4.3}$$

where the local WKB solutions ϕ_i are given in (4.1).

The expressions in (4.3) look rather formidable. As a consistency check and an application, we consider the exact quantization condition (EQC) for a spectral problem relevant to the SU(3) equation (1.12). Imagine we would like to study a certain bound state solution to (1.12) living along a one-dimensional path between $z = 0$ and $z = \infty$, where the solution decays as z approaches 0 and ∞. For example, suppose the one-dimensional path goes into $z = 0$ and $z = \infty$ along the negative imaginary axis, then the condition for the existence of such bound states is that the distinguished solution s decaying into $z = 0$ is proportional to the distinguished solution t decaying into $z = \infty$ after analytical continuation to a common region. Substituting this condition into (4.3), the complicated-looking expressions simplify to

$$\frac{1}{\mu_\beta} \mathcal{X}_{\gamma_3'} = 1, \quad \mu_\beta \mathcal{X}_{\gamma_4'} = 1. \tag{4.4}$$

Equation (4.4) is regarded as the EQC for such bound states.

In [61] the authors studied EQC for a family of exactly solvable deformed Hamiltonians obtained by quantizing the Seiberg-Witten curve for 4d $N = 2$ SU(N) SYM in the hyperelliptic form. In the case of SU(3) SYM, the Seiberg-Witten curve we use here comes from class S construction; it is in the dual parametrization of the Seiberg-Witten curve considered in [61]. It would be interesting to clarify the relation between (4.4) and the EQC in [61] derived from certain 4d limit of TS/ST correspondence.

4.4 The asymptotic behavior

Similar to section 3.5, here we perform numerical checks against the asymptotic behavior of spectral coordinates. Taking $u_1 = 4.5$, $u_2 = 0$ and $\Lambda = 1$, some numerical results for equation A and B of (1.12) are listed in table 5 and table 6 respectively.

In the evaluation of $\log \mathcal{X}_{\gamma'}$ using (4.2) and (4.3), similar to what happens in the strong coupling region, we found it difficult to perform numerical evaluation at small $\hbar$. Compared to the strong coupling region, here the numerical evaluation contains an extra step, namely diagonalizing the monodromy matrix M and finding its eigenvalues and eigenvectors. As $\hbar$ gets rather small, one of the eigenvalues for M becomes very small, introducing further difficulty in the numerical analysis. Nevertheless, from table 5 and table 6 one can see that as $\hbar$ goes from 1 to 0.7, $\hbar \log \mathcal{X}_{\gamma'}$ becomes closer to the truncated quantum periods expansion. This provides evidence for the conjectured asymptotic behavior of spectral coordinates.

	$\hbar = 1$		$\hbar = 0.7$	
	evaluation (4.2-4.3)	$\frac{1}{\hbar}\Pi_{\gamma'}(\hbar)$ at $o(\hbar^2)$	evaluation (4.2-4.3)	$\frac{1}{\hbar}\Pi_{\gamma'}(\hbar)$ at $o(\hbar^2)$
$\log\mathcal{X}_{\gamma'_1}$	11.90	11.98	18.14	18.17
$\log\mathcal{X}_{\gamma'_2}$	-11.90	-11.98	-18.14	-18.17
$\log\mathcal{X}_{\gamma'_3}$	$5.93 + 0.94i$	$5.99 + 0.96i$	$9.080 + 2.692i$	$9.086 + 2.697i$
$\log\mathcal{X}_{\gamma'_4}$	$-5.93 - 0.94i$	$-5.99 - 0.96i$	$-9.080 - 2.692i$	$-9.086 - 2.697i$

Table 5. Comparison of $\log\mathcal{X}_{\gamma'}$ with the formal quantum periods expansion up to order-$\hbar^2$ for equation A of (1.12) at $\hbar = 1$ and $\hbar = 0.7$, where we have set $u_1 = 4.5$, $u_2 = 0$ and $\Lambda = 1$.

	$\hbar = 1$		$\hbar = 0.7$	
	evaluation (4.2-4.3)	$\frac{1}{\hbar}\Pi_{\gamma'}(\hbar)$ at $o(\hbar^2)$	evaluation (4.2-4.3)	$\frac{1}{\hbar}\Pi_{\gamma'}(\hbar)$ at $o(\hbar^2)$
$\log\mathcal{X}_{\gamma'_1}$	13.411	13.408	19.1723	19.1715
$\log\mathcal{X}_{\gamma'_2}$	-13.411	-13.408	-19.1723	-19.1715
$\log\mathcal{X}_{\gamma'_3}$	$6.67 + 2.71i$	$6.71 + 2.66i$	$9.61 + 3.89i$	$9.59 + 3.88i$
$\log\mathcal{X}_{\gamma'_4}$	$-6.67 - 2.71i$	$-6.71 - 2.66i$	$-9.61 - 3.89i$	$-9.59 - 3.88i$

Table 6. Comparison of $\log\mathcal{X}_{\gamma'}$ with the formal quantum periods expansion up to order-$\hbar^2$ for equation B of (1.12) at $\hbar = 1$ and $\hbar = 0.7$, where we have set $u_1 = 4.5$, $u_2 = 0$ and $\Lambda = 1$.

Acknowledgments

References

[1] G. Alvarez and C. Casares, *Exponentially small corrections in the asymptotic expansion of the eigenvalues of the cubic anharmonic oscillator*, *J. Phys. A* **33** (2000) 5171.

[2] G. Alvarez and C. Casares, *Uniform asymptotic and jwkb expansions for anharmonic oscillators*, *J. Phys. A* **33** (2000) 2499.

[3] J. Zinn-Justin and U.D. Jentschura, *Multi-instantons and exact results II: Specific cases, higher-order effects, and numerical calculations*, *Annals Phys.* **313** (2004) 269 [quant-ph/0501137] [INSPIRE].

[4] J. Zinn-Justin and U.D. Jentschura, *Multi-instantons and exact results I: Conjectures, WKB expansions, and instanton interactions*, *Annals Phys.* **313** (2004) 197 [`quant-ph/0501136`] [INSPIRE].

[5] U.D. Jentschura, A. Surzhykov and J. Zinn-Justin, *Multi-instantons and exact results. III: Unification of even and odd anharmonic oscillators*, *Annals Phys.* **325** (2010) 1135 [`arXiv:1001.3910`] [INSPIRE].

[6] G.V. Dunne and M. Ünsal, *Generating nonperturbative physics from perturbation theory*, *Phys. Rev. D* **89** (2014) 041701 [`arXiv:1306.4405`] [INSPIRE].

[7] G. Basar, G.V. Dunne and M. Ünsal, *Resurgence theory, ghost-instantons, and analytic continuation of path integrals*, *JHEP* **10** (2013) 041 [`arXiv:1308.1108`] [INSPIRE].

[8] G.V. Dunne and M. Ünsal, *Uniform WKB, Multi-instantons, and Resurgent Trans-Series*, *Phys. Rev. D* **89** (2014) 105009 [`arXiv:1401.5202`] [INSPIRE].

[9] T. Misumi, M. Nitta and N. Sakai, *Resurgence in sine-Gordon quantum mechanics: Exact agreement between multi-instantons and uniform WKB*, *JHEP* **09** (2015) 157 [`arXiv:1507.00408`] [INSPIRE].

[10] A. Behtash, G.V. Dunne, T. Schäfer, T. Sulejmanpasic and M. Ünsal, *Toward Picard-Lefschetz theory of path integrals, complex saddles and resurgence*, *Ann. Math. Sci. Appl.* **02** (2017) 95 [`arXiv:1510.03435`] [INSPIRE].

[11] G.V. Dunne and M. Ünsal, *WKB and Resurgence in the Mathieu Equation*, `arXiv:1603.04924` [INSPIRE].

[12] T. Fujimori, S. Kamata, T. Misumi, M. Nitta and N. Sakai, *Exact resurgent trans-series and multibion contributions to all orders*, *Phys. Rev. D* **95** (2017) 105001 [`arXiv:1702.00589`] [INSPIRE].

[13] N. Sueishi, $1/\epsilon$ *problem in resurgence*, *PTEP* **2021** (2021) 013B01 [`arXiv:1912.03518`] [INSPIRE].

[14] N. Sueishi, S. Kamata, T. Misumi and M. Ünsal, *On exact-WKB analysis, resurgent structure, and quantization conditions*, *JHEP* **12** (2020) 114 [`arXiv:2008.00379`] [INSPIRE].

[15] N. Sueishi, S. Kamata, T. Misumi and M. Ünsal, *Exact-WKB, complete resurgent structure, and mixed anomaly in quantum mechanics on* S^1, *JHEP* **07** (2021) 096 [`arXiv:2103.06586`] [INSPIRE].

[16] N.A. Nekrasov and S.L. Shatashvili, *Quantization of Integrable Systems and Four Dimensional Gauge Theories*, in *16th International Congress on Mathematical Physics*, Prague Czechia (2009), pg. 265 [`arXiv:0908.4052`] [INSPIRE].

[17] L.F. Alday, D. Gaiotto and Y. Tachikawa, *Liouville Correlation Functions from Four-dimensional Gauge Theories*, *Lett. Math. Phys.* **91** (2010) 167 [`arXiv:0906.3219`] [INSPIRE].

[18] N. Nekrasov, A. Rosly and S. Shatashvili, *Darboux coordinates, Yang-Yang functional, and gauge theory*, *Nucl. Phys. B Proc. Suppl.* **216** (2011) 69 [`arXiv:1103.3919`] [INSPIRE].

[19] D. Gaiotto, *Opers and TBA*, `arXiv:1403.6137` [INSPIRE].

[20] A. Grassi, Y. Hatsuda and M. Mariño, *Topological Strings from Quantum Mechanics*, *Annales Henri Poincaré* **17** (2016) 3177 [`arXiv:1410.3382`] [INSPIRE].

[21] M. Mariño, *Spectral Theory and Mirror Symmetry*, *Proc. Symp. Pure Math.* **98** (2018) 259 [arXiv:1506.07757] [INSPIRE].

[22] N. Nekrasov, *BPS/CFT correspondence: non-perturbative Dyson-Schwinger equations and qq-characters*, *JHEP* **03** (2016) 181 [arXiv:1512.05388] [INSPIRE].

[23] G. Başar and G.V. Dunne, *Resurgence and the Nekrasov-Shatashvili limit: connecting weak and strong coupling in the Mathieu and Lamé systems*, *JHEP* **02** (2015) 160 [arXiv:1501.05671] [INSPIRE].

[24] A.-K. Kashani-Poor and J. Troost, *Pure $\mathcal{N} = 2$ super Yang-Mills and exact WKB*, *JHEP* **08** (2015) 160 [arXiv:1504.08324] [INSPIRE].

[25] S.K. Ashok, D.P. Jatkar, R.R. John, M. Raman and J. Troost, *Exact WKB analysis of $\mathcal{N} = 2$ gauge theories*, *JHEP* **07** (2016) 115 [arXiv:1604.05520] [INSPIRE].

[26] G. Basar, G.V. Dunne and M. Ünsal, *Quantum Geometry of Resurgent Perturbative/Nonperturbative Relations*, *JHEP* **05** (2017) 087 [arXiv:1701.06572] [INSPIRE].

[27] S. Codesido, M. Mariño and R. Schiappa, *Non-Perturbative Quantum Mechanics from Non-Perturbative Strings*, *Ann. Henri Poincaré* **20** (2019) 543 [arXiv:1712.02603] [INSPIRE].

[28] K. Ito, S. Kanno and T. Okubo, *Quantum periods and prepotential in $\mathcal{N} = 2$ SU(2) SQCD*, *JHEP* **08** (2017) 065 [arXiv:1705.09120] [INSPIRE].

[29] K. Ito, M. Mariño and H. Shu, *TBA equations and resurgent Quantum Mechanics*, *JHEP* **01** (2019) 228 [arXiv:1811.04812] [INSPIRE].

[30] I. Coman, E. Pomoni and J. Teschner, *From quantum curves to topological string partition functions*, arXiv:1811.01978 [INSPIRE].

[31] L. Hollands and A. Neitzke, *Exact WKB and abelianization for the T_3 equation*, *Commun. Math. Phys.* **380** (2020) 131 [arXiv:1906.04271] [INSPIRE].

[32] A. Grassi, J. Gu and M. Mariño, *Non-perturbative approaches to the quantum Seiberg-Witten curve*, *JHEP* **07** (2020) 106 [arXiv:1908.07065] [INSPIRE].

[33] K. Ito, T. Kondo, K. Kuroda and H. Shu, *ODE/IM correspondence for affine Lie algebras: A numerical approach*, *J. Phys. A* **54** (2021) 044001 [arXiv:2004.09856] [INSPIRE].

[34] S. Jeong and N. Nekrasov, *Riemann-Hilbert correspondence and blown up surface defects*, *JHEP* **12** (2020) 006 [arXiv:2007.03660] [INSPIRE].

[35] N. Haouzi and J. Oh, *On the Quantization of Seiberg-Witten Geometry*, *JHEP* **01** (2021) 184 [arXiv:2004.00654] [INSPIRE].

[36] N. Lee and N. Nekrasov, *Quantum spin systems and supersymmetric gauge theories. Part I*, *JHEP* **03** (2021) 093 [arXiv:2009.11199] [INSPIRE].

[37] I. Coman, P. Longhi and J. Teschner, *From quantum curves to topological string partition functions II*, arXiv:2004.04585 [INSPIRE].

[38] K. Imaizumi, *Quantum periods and TBA equations for $\mathcal{N} = 2$ SU(2) $N_f = 2$ SQCD with flavor symmetry*, *Phys. Lett. B* **816** (2021) 136270 [arXiv:2103.02248] [INSPIRE].

[39] S. Jeong, N. Lee and N. Nekrasov, *Intersecting defects in gauge theory, quantum spin chains, and Knizhnik-Zamolodchikov equations*, *JHEP* **10** (2021) 120 [arXiv:2103.17186] [INSPIRE].

[40] N. Seiberg and E. Witten, *Electric-magnetic duality, monopole condensation, and confinement in $N = 2$ supersymmetric Yang-Mills theory*, *Nucl. Phys. B* **426** (1994) 19 [*Erratum ibid.* **430** (1994) 485] [`hep-th/9407087`] [ɪɴSPIRE].

[41] N. Seiberg and E. Witten, *Monopoles, duality and chiral symmetry breaking in $N = 2$ supersymmetric QCD*, *Nucl. Phys. B* **431** (1994) 484 [`hep-th/9408099`] [ɪɴSPIRE].

[42] G. Aminov, A. Grassi and Y. Hatsuda, *Black Hole Quasinormal Modes and Seiberg-Witten Theory*, `arXiv:2006.06111` [ɪɴSPIRE].

[43] G. Bonelli, C. Iossa, D.P. Lichtig and A. Tanzini, *Exact solution of Kerr black hole perturbations via CFT2 and instanton counting: Greybody factor, quasinormal modes, and Love numbers*, *Phys. Rev. D* **105** (2022) 044047 [`arXiv:2105.04483`] [ɪɴSPIRE].

[44] M. Bianchi, D. Consoli, A. Grillo and J.F. Morales, *QNMs of branes, BHs and fuzzballs from quantum SW geometries*, *Phys. Lett. B* **824** (2022) 136837 [`arXiv:2105.04245`] [ɪɴSPIRE].

[45] M. Bianchi, D. Consoli, A. Grillo and J.F. Morales, *More on the SW-QNM correspondence*, *JHEP* **01** (2022) 024 [`arXiv:2109.09804`] [ɪɴSPIRE].

[46] S. Jeong and N. Nekrasov, *Opers, surface defects, and Yang-Yang functional*, *Adv. Theor. Math. Phys.* **24** (2020) 1789 [`arXiv:1806.08270`] [ɪɴSPIRE].

[47] S. Jeong and F. Yan, *Exact WKB and the quantum Seiberg-Witten curve for $4d$ $N = 2$ pure SU(3) Yang-Mills, Part II: integral equations, instantons and surface defects*, work in progress.

[48] N.A. Nekrasov and S.L. Shatashvili, *Supersymmetric vacua and Bethe ansatz*, *Nucl. Phys. B Proc. Suppl.* **192-193** (2009) 91 [`arXiv:0901.4744`] [ɪɴSPIRE].

[49] N.A. Nekrasov and S.L. Shatashvili, *Quantum integrability and supersymmetric vacua*, *Prog. Theor. Phys. Suppl.* **177** (2009) 105 [`arXiv:0901.4748`] [ɪɴSPIRE].

[50] N.A. Nekrasov, *Seiberg-Witten prepotential from instanton counting*, *Adv. Theor. Math. Phys.* **7** (2003) 831 [`hep-th/0206161`] [ɪɴSPIRE].

[51] N. Nekrasov and A. Okounkov, *Seiberg-Witten theory and random partitions*, *Prog. Math.* **244** (2006) 525 [`hep-th/0306238`] [ɪɴSPIRE].

[52] D. Gaiotto, G.W. Moore and A. Neitzke, *Wall-crossing, Hitchin Systems, and the WKB Approximation*, `arXiv:0907.3987` [ɪɴSPIRE].

[53] D. Gaiotto, *$N = 2$ dualities*, *JHEP* **08** (2012) 034 [`arXiv:0904.2715`] [ɪɴSPIRE].

[54] N. Nekrasov and E. Witten, *The Omega Deformation, Branes, Integrability, and Liouville Theory*, *JHEP* **09** (2010) 092 [`arXiv:1002.0888`] [ɪɴSPIRE].

[55] N.J. Hitchin, *Stable bundles and integrable systems*, *Duke Math. J.* **54** (1987) 91 [ɪɴSPIRE].

[56] A. Beilinson and V. Drinfeld, *Opers*, `math/0501398`.

[57] W. Fenchel, J. Nielsen and A.L. Schmidt, *Discontinuous Groups of Isometries in the Hyperbolic Plane*, De Gruyter, Berlin Germany (2011).

[58] L. Hollands and O. Kidwai, *Higher length-twist coordinates, generalized Heun's opers, and twisted superpotentials*, *Adv. Theor. Math. Phys.* **22** (2018) 1713 [`arXiv:1710.04438`] [ɪɴSPIRE].

[59] S. Codesido, A. Grassi and M. Mariño, *Spectral Theory and Mirror Curves of Higher Genus*, *Annales Henri Poincaré* **18** (2017) 559 [`arXiv:1507.02096`] [ɪɴSPIRE].

[60] S.H. Katz, A. Klemm and C. Vafa, *Geometric engineering of quantum field theories*, *Nucl. Phys. B* **497** (1997) 173 [`hep-th/9609239`] [ɪɴSPIRE].

[61] A. Grassi and M. Mariño, *A Solvable Deformation of Quantum Mechanics*, *SIGMA* **15** (2019) 025 [`arXiv:1806.01407`] [ɪɴSPIRE].

[62] P.C. Argyres and A.E. Faraggi, *The vacuum structure and spectrum of N = 2 supersymmetric SU(n) gauge theory*, *Phys. Rev. Lett.* **74** (1995) 3931 [`hep-th/9411057`] [ɪɴSPIRE].

[63] A. Klemm, W. Lerche, S. Yankielowicz and S. Theisen, *Simple singularities and N = 2 supersymmetric Yang-Mills theory*, *Phys. Lett. B* **344** (1995) 169 [`hep-th/9411048`] [ɪɴSPIRE].

[64] A. Klemm, W. Lerche and S. Theisen, *Nonperturbative effective actions of N = 2 supersymmetric gauge theories*, *Int. J. Mod. Phys. A* **11** (1996) 1929 [`hep-th/9505150`] [ɪɴSPIRE].

[65] K. Ito and H. Shu, *ODE/IM correspondence and the Argyres-Douglas theory*, *JHEP* **08** (2017) 071 [`arXiv:1707.03596`] [ɪɴSPIRE].

[66] K. Ito and H. Shu, *TBA equations for the Schrödinger equation with a regular singularity*, *J. Phys. A* **53** (2020) 335201 [`arXiv:1910.09406`] [ɪɴSPIRE].

[67] D. Dumas and A. Neitzke, *Opers and nonabelian Hodge: numerical studies*, `arXiv:2007.00503` [ɪɴSPIRE].

[68] O. Dumitrescu, L. Fredrickson, G. Kydonakis, R. Mazzeo, M. Mulase and A. Neitzke, *Opers versus nonabelian Hodge*, `arXiv:1607.02172` [ɪɴSPIRE].

[69] D. Gaiotto, G.W. Moore and A. Neitzke, *Spectral networks*, *Annales Henri Poincaré* **14** (2013) 1643 [`arXiv:1204.4824`] [ɪɴSPIRE].

[70] A. Mironov and A. Morozov, *Nekrasov Functions and Exact Bohr-Zommerfeld Integrals*, *JHEP* **04** (2010) 040 [`arXiv:0910.5670`] [ɪɴSPIRE].

[71] W. He and Y.-G. Miao, *Mathieu equation and Elliptic curve*, *Commun. Theor. Phys.* **58** (2012) 827 [`arXiv:1006.5185`] [ɪɴSPIRE].

[72] M.-x. Huang, *On Gauge Theory and Topological String in Nekrasov-Shatashvili Limit*, *JHEP* **06** (2012) 152 [`arXiv:1205.3652`] [ɪɴSPIRE].

[73] A. Grassi, Q. Hao and A. Neitzke, *Exact WKB methods in* SU(2) $N_f = 1$, *JHEP* **01** (2022) 046 [`arXiv:2105.03777`] [ɪɴSPIRE].

[74] R. Balian, G. Parisi and A. Voros, *Quartic oscillator*, in *Feynman path integrals*, *Lect. Notes Phys.* **106** (1979) 1.

[75] S. Codesido and M. Mariño, *Holomorphic Anomaly and Quantum Mechanics*, *J. Phys. A* **51** (2018) 055402 [`arXiv:1612.07687`] [ɪɴSPIRE].

[76] I. Aniceto, G. Basar and R. Schiappa, *A Primer on Resurgent Transseries and Their Asymptotics*, *Phys. Rept.* **809** (2019) 1 [`arXiv:1802.10441`] [ɪɴSPIRE].

[77] L. Hollands and A. Neitzke, *Spectral Networks and Fenchel–Nielsen Coordinates*, *Lett. Math. Phys.* **106** (2016) 811 [`arXiv:1312.2979`] [ɪɴSPIRE].

[78] V.V. Fock and A.B. Goncharov, *Moduli spaces of local systems and higher Teichmuller theory*, `math/0311149`.

[79] N. Nikolaev, *Abelianisation of logarithmic $\mathfrak{sl}_2$-connections*, *Sel. Math. New Ser.* **27** (2021) 78 [`arXiv:1902.03384`].

[80] D.G.L. Allegretti, *Voros symbols as cluster coordinates*, *J. Topol.* **12** (2019) 1031 [`arXiv:1802.05479`] [INSPIRE].

[81] D.G.L. Allegretti, *On the wall-crossing formula for quadratic differentials*, `arXiv:2006.08059` [INSPIRE].

[82] D. Gaiotto, G.W. Moore and A. Neitzke, *Four-dimensional wall-crossing via three-dimensional field theory*, *Commun. Math. Phys.* **299** (2010) 163 [`arXiv:0807.4723`] [INSPIRE].

[83] M. Kontsevich and Y. Soibelman, *Stability structures, motivic Donaldson-Thomas invariants and cluster transformations*, `arXiv:0811.2435` [INSPIRE].

[84] M. Matone, *Instantons and recursion relations in $N = 2$ SUSY gauge theory*, *Phys. Lett. B* **357** (1995) 342 [`hep-th/9506102`] [INSPIRE].

[85] A.S. Losev, A. Marshakov and N.A. Nekrasov, *Small instantons, little strings and free fermions*, in *From Fields to Strings: Circumnavigating Theoretical Physics: A Conference in Tribute to Ian Kogan*, Oxford U.K. (2003), pg. 581 [`hep-th/0302191`] [INSPIRE].

[86] R. Flume, F. Fucito, J.F. Morales and R. Poghossian, *Matone's relation in the presence of gravitational couplings*, *JHEP* **04** (2004) 008 [`hep-th/0403057`] [INSPIRE].

[87] M. Aganagic, M.C.N. Cheng, R. Dijkgraaf, D. Krefl and C. Vafa, *Quantum Geometry of Refined Topological Strings*, *JHEP* **11** (2012) 019 [`arXiv:1105.0630`] [INSPIRE].

[88] F. Fucito, J.F. Morales and R. Poghossian, *Wilson loops and chiral correlators on squashed spheres*, *JHEP* **11** (2015) 064 [`arXiv:1507.05426`] [INSPIRE].

[89] M. Bullimore, H.-C. Kim and P. Koroteev, *Defects and Quantum Seiberg-Witten Geometry*, *JHEP* **05** (2015) 095 [`arXiv:1412.6081`] [INSPIRE].

[90] K.K. Kozlowski and J. Teschner, *TBA for the Toda chain*, `arXiv:1006.2906` [INSPIRE].

[91] D. Gaiotto, *Asymptotically free $\mathcal{N} = 2$ theories and irregular conformal blocks*, *J. Phys. Conf. Ser.* **462** (2013) 012014 [`arXiv:0908.0307`] [INSPIRE].

[92] A. Marshakov, A. Mironov and A. Morozov, *On non-conformal limit of the AGT relations*, *Phys. Lett. B* **682** (2009) 125 [`arXiv:0909.2052`] [INSPIRE].

[93] A. Mironov and A. Morozov, *On AGT relation in the case of* U(3), *Nucl. Phys. B* **825** (2010) 1 [`arXiv:0908.2569`] [INSPIRE].

[94] A. Mironov and A. Morozov, *Nekrasov Functions from Exact BS Periods: The Case of* SU(N), *J. Phys. A* **43** (2010) 195401 [`arXiv:0911.2396`] [INSPIRE].

[95] N. Wyllard, *A(N − 1) conformal Toda field theory correlation functions from conformal $N = 2$ SU(N) quiver gauge theories*, *JHEP* **11** (2009) 002 [`arXiv:0907.2189`] [INSPIRE].

[96] L.F. Alday, D. Gaiotto, S. Gukov, Y. Tachikawa and H. Verlinde, *Loop and surface operators in $N = 2$ gauge theory and Liouville modular geometry*, *JHEP* **01** (2010) 113 [`arXiv:0909.0945`] [INSPIRE].

[97] K. Maruyoshi and M. Taki, *Deformed Prepotential, Quantum Integrable System and Liouville Field Theory*, *Nucl. Phys. B* **841** (2010) 388 [arXiv:1006.4505] [INSPIRE].

[98] R. Poghossian, *Deforming SW curve*, *JHEP* **04** (2011) 033 [arXiv:1006.4822] [INSPIRE].

[99] A. Popolitov, *On relation between Nekrasov functions and BS periods in pure* SU(N) *case*, arXiv:1001.1407 [INSPIRE].

[100] Y. Zenkevich, *Nekrasov prepotential with fundamental matter from the quantum spin chain*, *Phys. Lett. B* **701** (2011) 630 [arXiv:1103.4843] [INSPIRE].

[101] D. Fioravanti, H. Poghosyan and R. Poghossian, *T, Q and periods in* SU(3) $\mathcal{N} = 2$ *SYM*, *JHEP* **03** (2020) 049 [arXiv:1909.11100] [INSPIRE].

[102] A. Voros, *The return of the quartic oscillator. the complex WKB method*, *Ann. Henri Poincaré* **39** (1983) 211.

[103] H.J. Silverstone, *JWKB connection-formula problem revisited via Borel summation*, *Phys. Rev. Lett.* **55** (1985) 2523.

[104] E. Delabaere, H. Dillinger and F. Pham, *Exact semiclassical expansions for one-dimensional quantum oscillators*, *J. Math. Phys.* **38** (1997) 6126.

[105] T. Kawai and Y. Takei, *Algebraic analysis of singular perturbation theory*, (Translations of Mathematical Monographs 227), *Bull. Lond. Math. Soc.* **40** (2008) 723.

[106] K. Iwaki and T. Nakanishi, *Exact WKB analysis and cluster algebras*, arXiv:1401.7094.

[107] T. Aoki, T. Kawai and Y. Takei, *New Turning Points in the Exact WKB Analysis for Higher-order Ordinary Differential Equations*, Technical Report, Research Institute for Mathematical Sciences, Kyoto University, Kyoto Japan (1991).

[108] T. Aoki, T. Kawai, S. Sasaki, A. Shudo and Y. Takei, *Virtual turning points and bifurcation of stokes curves for higher order ordinary differential equations*, *J. Phys. A* **38** (2005) 3317.

[109] A. Shudo and K.S. Ikeda, *Stokes geometry for the quantum Hénon map*, *Nonlinearity* **21** (2008) 1831.

[110] N. Honda, T. Kawai and Y. Takei, *Virtual turning points*, *SpringerBriefs in mathematical physics*, Springer, Tokyo Japan (2015).

[111] S. Sasaki, *A bifurcation phenomenon of stokes curves around a double turning point, and influence of virtual turning points upon the transition probabilities for three-level systems*, *Adv. Math.* **301** (2016) 711.

[112] N. Nikolaev, *Existence and Uniqueness of Exact WKB Solutions for Second-Order Singularly Perturbed Linear ODEs*, arXiv:2106.10248.

[113] Y. Kabaya, *Parametrization of psl(2, c)-representations of surface groups*, arXiv:1110.6674.

[114] M. Alim, S. Cecotti, C. Cordova, S. Espahbodi, A. Rastogi and C. Vafa, $\mathcal{N} = 2$ *quantum field theories and their BPS quivers*, *Adv. Theor. Math. Phys.* **18** (2014) 27 [arXiv:1112.3984] [INSPIRE].

[115] D. Galakhov, P. Longhi, T. Mainiero, G.W. Moore and A. Neitzke, *Wild Wall Crossing and BPS Giants*, *JHEP* **11** (2013) 046 [arXiv:1305.5454] [INSPIRE].

[116] M. Cirafici and M. Del Zotto, *Discrete Integrable Systems, Supersymmetric Quantum Mechanics, and Framed BPS States — I*, arXiv:1703.04786 [INSPIRE].